C-type natriuretic peptide activates a non-selective cation current in acutely isolated rat cardiac fibroblasts via natriuretic peptide C receptor-mediated signalling

R. A. Rose[1], N. Hatano[1], S. Ohya[2], Y. Imaizumi[2] and W. R. Giles[1,3]

[1]*Department of Physiology and Biophysics, Faculty of Medicine, University of Calgary, Calgary, Alberta, Canada T2N 4N1*
[2]*Department of Molecular and Cellular Pharmacology, Nagoya City University, Nagoya 467-8603, Japan*
[3]*Faculty of Kinesiology, University of Calgary, Alberta, Canada*

In the heart, fibroblasts play an essential role in the deposition of the extracellular matrix and they also secrete a number of hormonal factors. Although natriuretic peptides, including C-type natriuretic peptide (CNP) and brain natriuretic peptide, have antifibrotic effects on cardiac fibroblasts, the effects of CNP on fibroblast electrophysiology have not been examined. In this study, acutely isolated ventricular fibroblasts from the adult rat were used to measure the effects of CNP (2×10^{-8} M) under whole-cell voltage-clamp conditions. CNP, as well as the natriuretic peptide C receptor (NPR-C) agonist cANF (2×10^{-8} M), significantly increased an outwardly rectifying non-selective cation current (NSCC). This current has a reversal potential near 0 mV. Activation of this NSCC by cANF was abolished by pre-treating fibroblasts with pertussis toxin, indicating the involvement of G_i proteins. The cANF-activated NSCC was inhibited by the compounds Gd^{3+}, SKF 96365 and 2-aminoethoxydiphenyl borate. Quantitative RT-PCR analysis of mRNA from rat ventricular fibroblasts revealed the expression of several transient receptor potential (TRP) channel transcripts. Additional electrophysiological analysis showed that U73122, a phospholipase C antagonist, inhibited the cANF-activated NSCC. Furthermore, the effects of CNP and cANF were mimicked by the diacylglycerol analogue 1-oleoyl-2-acetyl-*sn*-glycerol (OAG), independently of protein kinase C activity. These are defining characteristics of specific TRPC channels. More detailed molecular analysis confirmed the expression of full-length TRPC2, TRPC3 and TRPC5 transcripts. These data indicate that CNP, acting via the NPR-C receptor, activates a NSCC that is at least partially carried by TRPC channels in cardiac fibroblasts.

(Resubmitted 9 September 2006; accepted after revision 22 December 2006; first published online 4 January 2007)
Corresponding author W. R. Giles: Faculty of Kinesiology, University of Calgary, 2500 University Drive, Calgary, AB, Canada T2N 1N4. Email: wgiles@ucalgary.ca

In the heart, fibroblasts comprise approximately 90% of the non-myocyte cell population and are responsible for the synthesis and secretion of various extracellular matrix proteins including collagen (types I and II) and matrix metalloproteinases (Brilla & Maisch, 1994; Baudino *et al.* 2006). Cardiac fibrosis, which is characterized by the abnormal proliferation of interstitial fibroblasts and an increase in the deposition of collagen, results in increased myocardial stiffness and diastolic dysfunction (Brilla & Maisch, 1994). In this way, fibroblasts can play a major role in the remodelling of the myocardium that can contribute to conduction disturbances and mechanical compromise in the setting of heart failure (Brilla & Maisch, 1994; Brilla *et al.* 1995).

In addition to their role in maintaining the extracellular matrix, fibroblasts secrete a wide variety of hormonal factors, which then act as both autocrine and paracrine signals in the myocardium (Brilla *et al.* 1995; Ellmers *et al.* 2002). For example, cardiac fibroblasts secrete natriuretic peptides including brain natriuretic peptide and C-type natriuretic peptide (CNP). These peptides may have antifibrotic and antiproliferative functions in the heart (Tsuruda *et al.* 2002; Horio *et al.* 2003; Kapoun *et al.* 2004; Kawakami *et al.* 2004; Huntley *et al.* 2006).

In many different tissues, including the heart, the physiological effects of natriuretic peptides are initiated by the binding of two types of cell surface receptors. The natriuretic peptide type A and B receptors (NPR-A and NPR-B) include particulate guanylyl cyclase domains and, as a consequence, can alter intracellular cGMP levels when the peptide is bound to the receptor (Maack, 1992; Lucas *et al.* 2000). In contrast, the natriuretic peptide C receptor

 DOI: 10.1113/jphysiol.2006.120832

(NPR-C) is functionally linked to the G protein G_i, which inhibits adenylyl cyclase activity (Anand-Srivastava *et al.* 1996; Pagano & Anand-Srivastava, 2001; Zhou & Murthy, 2003). NPR-C, which may comprise up to 95% of the total NPR population (Maack, 1992), is known to bind all the natriuretic peptides with similar affinity (Levin *et al.* 1998) and is expressed in cardiac fibroblasts (Huntley *et al.* 2006).

Recently, we characterized a novel role for NPR-C in the CNP-mediated inhibition of L-type Ca^{2+} current in cardiac myocytes (Rose *et al.* 2003, 2004); however, the electrophysiological effects of CNP on the cardiac fibroblast have not been identified. As the fibroblast is considered a classic example of a non-excitable cell (Allessie *et al.* 2005), we reasoned that transient receptor potential (TRP) cation channel(s) may play a role in mediating electrophysiological effects of CNP. TRP channels are known to mediate influxes of ions, including Na^+, Ca^{2+}, K^+ and Mg^{2+} (depending on the specific TRP channel), in a variety of cell types (Clapham *et al.* 2001; Clapham, 2003; Nilius *et al.* 2005).

Our findings demonstrate that (i) cardiac fibroblasts express non-selective cation channels that are potently activated by CNP, (ii) the effects of CNP are mediated by the NPR-C receptor and the activation of G_i, and (iii) the CNP/NPR-C-activated non-selective cation current is due to the activation of one or more TRPC cation channels.

Methods

Isolation of cardiac fibroblasts

All procedures used in this study were in compliance with the Canadian Council on Animal Care guidelines and were approved by the University of Calgary Animal Resource Centre.

Fibroblasts (and myocytes) were isolated from the ventricles of adult rats as previously described (Chilton *et al.* 2005). In summary, male Sprague-Dawley rats were anaesthetized using isoflurane inhalation so that no paw pinch reflex could be elicited, and then they were killed by cervical dislocation. Following this, the hearts were excised into ice-cold Tyrode solution containing (mM): 140 NaCl, 5.4 KCl, 1 $CaCl_2$, 1 $MgCl_2$, 10 Hepes, 5.5 glucose. The pH was adjusted to 7.4 with NaOH. The heart was Langendorff-perfused retrogradely via the aorta at 8 ml min^{-1} with three successive solutions: (1) Tyrode solution for 5 min, (2) Ca^{2+}-free Tyrode solution for 5 min, and (3) a Tyrode solution containing 4 μM $CaCl_2$, 0.04 mg ml^{-1} collagenase type II, and 0.004 mg ml^{-1} protease XIV, for 8 min. The ventricles were then removed from the rest of the heart and cut into pieces approximately 1 mm^3 in size. These were further digested in Tyrode solution containing 10 μM $CaCl_2$, 1 mg ml^{-1} collagenase type II, 0.1 mg ml^{-1} protease XIV, and 0.5% bovine serum albumin, in a shaker bath at 37°C. Small samples of this mixture were observed periodically for the appearance of single myocytes and fibroblasts. It was typically after 35–40 min in the shaker bath that aliquots of cell suspension were taken and placed in a KB solution consisting of (mM): 100 potassium glutamate, 10 potassium aspartate, 25 KCl, 10 KH_2PO_4, 2 $MgSO_4$, 20 taurine, 5 creatine, 0.5 EGTA, 20 glucose, 5 Hepes, and 0.1% bovine serum albumin (pH adjusted to 7.2 with KOH). Cells were left in this solution for approximately 1 h before being used for electrophysiological studies. Fibroblasts were easily distinguished from myocytes by their much smaller size and more spherical shape (Chilton *et al.* 2005; Shibukawa *et al.* 2005).

Electrophysiology

The whole-cell configuration of the patch-clamp technique (Hamill *et al.* 1981) was used for voltage-clamp studies of single rat cardiac fibroblasts. Micropipettes were pulled from borosilicate glass (with filament, 1.5 mm o.d., 0.86 mm i.d.; Sutter Instrument Company) using a Flaming/Brown pipette puller (model P-87; Sutter Instrument Company). The resistance of these pipettes was 5–10 MΩ when filled with recording solution.

Microelectrodes were positioned with a hydraulic micromanipulator (SD Instruments) mounted on the stage of an inverted microscope (Nikon Diaphot). Seal resistances were 2–15 GΩ. Rupturing the cell membrane in the patch resulted in access resistances of 5–15 MΩ. The membrane capacitance of rat ventricular cardiac fibroblasts was small (4–15 pF). Series resistance compensation was not typically used since agonist-induced currents were relatively small and no transient responses were analysed in detail. Some of the data presented in Figs 1 and 2 were acquired using the perforated-patch-clamp technique. This was achieved by including amphotericin B (300 μg ml^{-1}) in the pipette solution. Results were not different from those obtained using whole-cell recordings and were therefore combined.

Voltage-clamp command waveforms and the resulting capacitative and ionic current changes were acquired using an Axoclamp 200B amplifier, a Digidata 1322A digitizer and pCLAMP 8 software (all from Axon Instruments). Data were stored for analysis offline.

When attempting to measure L-type Ca^{2+} current ($I_{Ca(L)}$), fibroblasts were held at –80 mV. A prepulse to –50 mV for 250 ms, and then a test pulse to 0 mV for 250 ms were applied. The prepulse was to inactivate any other voltage-gated currents that may have been present, such as I_{Na}. To measure non-selective cation currents, fibroblasts were held at 0 mV. Ramp voltage clamp waveforms from –100 to +100 mV were applied over 1 s. In some experiments, step protocols were used. In these experiments, cells were held at 0 mV and then given a series of 500 ms voltage-clamp steps from –100 to +100 mV in 20 mV increments.

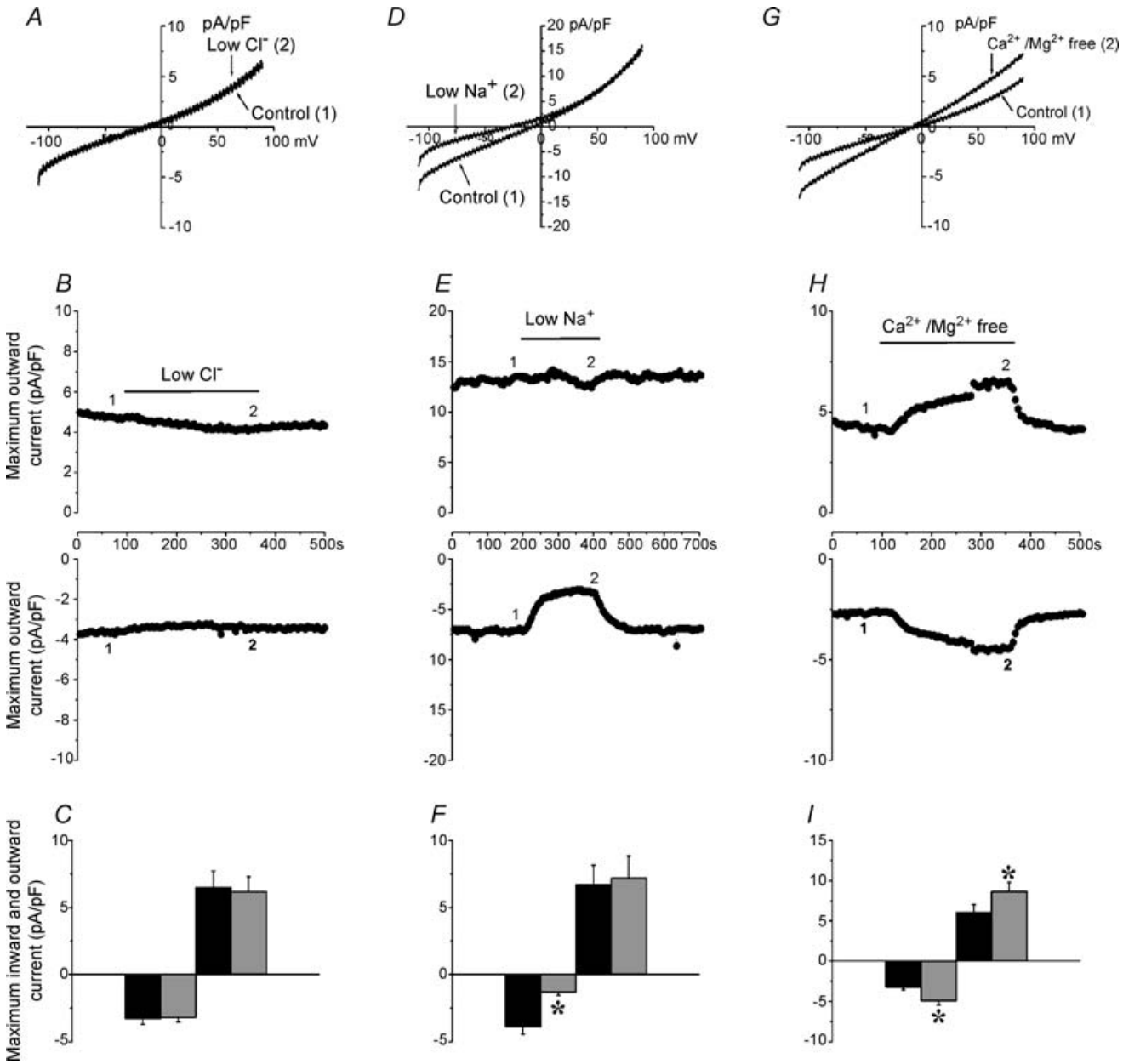

Figure 1. Properties of a weakly outwardly rectifying ionic current identified using voltage ramps in acutely isolated rat cardiac fibroblasts

The voltage-clamp protocol consisted of a 1 s ramp from −100 to +100 mV from a holding potential of 0 mV. Under these conditions, and in the absence of any external pharmacological compounds, a small weakly outwardly rectifying current was identified. *A* and *B*, representative recordings and time-course data (at −100 and +100 mV) of the effects of replacing external Cl^- with $CH_3SO_3^-$. *C*, summary data (mean ± S.E.M.; $n = 6$ fibroblasts) for control conditions (black bars) and external Cl^- replacement (shaded bars) at −100 and +100 mV. There was no significant effect of external Cl^- replacement on this current indicating that it is not a Cl^- conductance. *D* and *E*, representative recordings and time-course data of the effects of replacing external Na^+ with $NMDG^+$. *F*, summary data (mean ± S.E.M.; $n = 10$ fibroblasts) for control conditions and external Na^+ replacement. Replacement of external Na^+ with $NMDG^+$ significantly decreased inward current at −100 mV without altering outward current at +100 mV. As shown in the time-course data, this effect was completely reversible following a return to Na^+-containing superfusate. *G* and *H*, representative recordings and the time course of the effects of divalent cation removal. *I*, summary data (mean ± S.E.M.; $n = 9$ fibroblasts) for the effects of removing external Ca^{2+} and Mg^{2+}. Note that divalent cation removal significantly increased both inward and outward currents and linearized the current–voltage (*I–V*) curve. As shown in the time-course data, this effect was completely reversible.

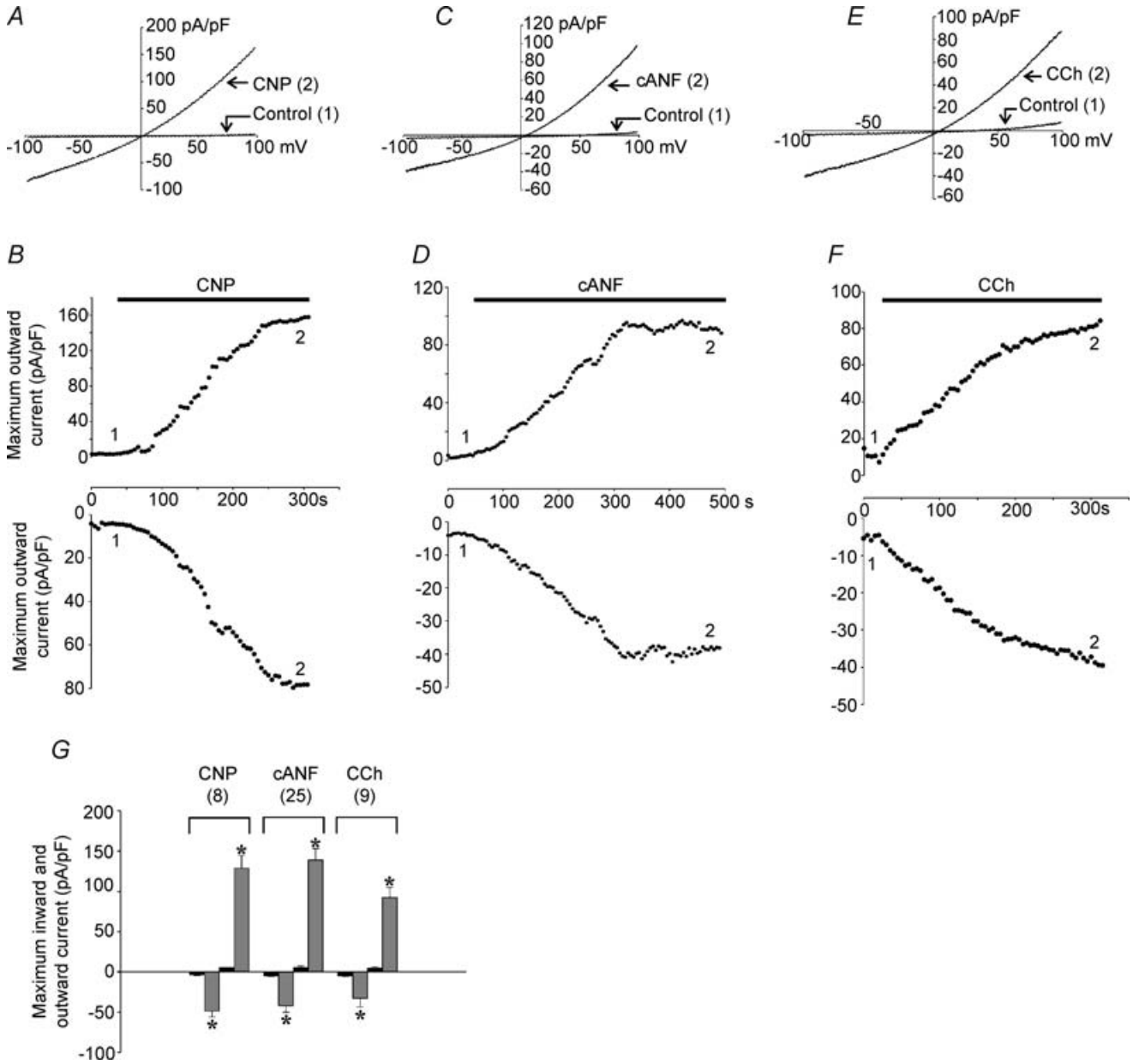

Figure 2. CNP (2×10^{-8} M) and the NPR-C agonist, cANF (2×10^{-8} M), increase a non-selective cation current in acutely isolated rat cardiac fibroblasts

Currents were elicited by 1 s voltage ramps from −100 to +100 mV from a holding potential of 0 mV. *A* and *B*, representative recordings and time-course data for the effects of C-type natriuretic peptide (CNP) on the non-selective cation current (NSCC). The representative traces for control conditions (1) and CNP treatment (2) correspond to the points indicated in the time-course figure. Note that CNP significantly increased the weakly outwardly rectifying NSCC. *C* and *D*, representative recordings and time-course data for the effects of cANF, a selective agonist for the natriuretic peptide C receptor (NPR-C) that activates G_i proteins, on the NSCC. Note that cANF mimics the effect of CNP on isolated rat cardiac fibroblasts, suggesting the effect of CNP is via the NPR-C receptor. *E* and *F*, representative recordings and time-course data for the effects of carbachol (CCh, 1×10^{-5} M) on the NSCC. CCh, which activates G_i proteins via M2 muscarinic receptors, elicits a similar effect to CNP and cANF. Summary data (mean ± S.E.M.) for the effects of CNP, cANF and CCh (*n* values shown in parentheses) on maximum inward and outward current are shown in *G*. In these histograms, black bars are control conditions, and shaded bars represent drug treatment. Each compound significantly (*) increased inward and outward current at −100 and +100 mV, respectively ($P < 0.05$) compared with control conditions. There was no significant difference between the effects of CNP, cANF or CCh ($P > 0.05$) on the NSCC in rat ventricular fibroblasts.

Solutions and drugs

The recording chamber was superfused at 22–23°C with a modified Tyrode solution, containing the following (mM): 140 NaCl, 5.4 TEA-Cl, 2 $CaCl_2$, 1 $MgCl_2$, 10 Hepes, 1 glucose. The pH was adjusted to 7.4 using CsOH. The pipette solution contained the following (mM): 135 CsCl, 0.1 $CaCl_2$, 10 EGTA, 4 MgATP, 1 $MgCl_2$, 10 Hepes, 6.6 sodium phosphocreatine, and 0.3 GTP (sodium salt). The pH was adjusted to 7.4 with CsOH. The free Ca^{2+} concentration of this solution was nominally zero. All pharmacological compounds used in this study were purchased from Sigma Chemical Company, with the exception of CNP and the NPR-C-selective agonist, cANF, which were purchased from Peninsula Laboratories.

PCR

Cardiac fibroblasts were acutely isolated as described above and approximately 100 000 cells were collected using a cell sorter. Total RNA extraction and reverse-transcription from these fibroblasts were performed as previously reported (Ohya *et al.* 2002; Muraki *et al.* 2003). Reverse transcription (RT) was performed according to Invitrogen's protocol. In brief, total RNA (2 μg) and 200 ng of random hexamer in RNase-free H_2O were heated for 10 min at 70°C and incubated for 10 min at 25°C for annealing. This sample was incubated for 60 min at 42°C using 150 units Superscript II RNase H^- reverse transcriptase (Invitrogen) in a solution (final volume 20 μl) that contained 50 mM Tris-HCl (pH 8.3), 40 mM KCl, 6 mM $MgCl_2$, 1 mM DTT, and 1 mM individual dNTPs. After this RT procedure, the reaction mixture was added to 80 μl of distilled water and used for PCR. The PCR amplification profile was as follows: 15 s at 95°C and 60 s at 60°C for 1 min, according to a user protocol of AmpliTaq Gold (Applied Biosystems, Foster City, CA, USA). The amplification was performed for 35 cycles. Glyceraldehyde-3-phosphate dehydrogenase (GAPDH) primers were used to confirm that the products generated were representative of RNA. The amplified products were separated by electrophoresis on a 2.5% agarose/1× TAE (Tris, acetic acid, EDTA) gel, and the DNA bands were visualized by ethidium bromide staining. Each amplified product was sequenced by the chain termination method with an ABI PRISM 3100 genetic analyser (Applied Biosystems). Negative controls were carried out using water instead of reverse transcriptase, which resulted in no detectable signals in the PCR reaction. Brain cDNA was used as the positive control.

Real-time quantitative PCR was performed with the use of Syber Green chemistry on an ABI 7000 sequence detector (Applied Biosystems). Unknown quantities relative to the standard curve for a particular set of primers were calculated, yielding transcriptional quantification of gene products relative to the endogenous standard (GAPDH).

For the initial screening of TRP channel transcripts (Fig. 4) the following PCR primers were used: TRPC1 (NM_053558, 612–712), amplicon = 101 bp; TRPC2 (NM_022638, 991–1098), amplicon = 108 bp; TRPC3 (NM_021771, 1453–1557), amplicon = 105 bp; TRPC4 (NM_080396, 1009–1116), amplicon = 108 bp; TRPC5 (NM_080898, 197–1399), amplicon = 103 bp; TRPC6 (NM_053559, 1386–1486), amplicon = 101 bp; TRPC7 (XM_225159, 1536–1638), amplicon = 103 bp; TRPV1 (NM_031982, 1976–2076), amplicon = 101 bp; TRPV2 (NM_017207, 1889–1989), amplicon = 101 bp; TRPV3 homologue (NW_047336, 1156467–1156520), amplicon = 104 bp; TRPV4 (NM_023970, 1097–1204), amplicon = 108 bp; TRPV5 (AF209196, 1473–1573), amplicon = 101 bp; TRPV6 (NM_053686, 1871–1971), amplicon = 101 bp; TRPM1 (XM_341869, 1220–1320) amplicon = 101 bp; TRPM3 (XM_342035, 517–617), amplicon = 101 bp; TRPM4 (AB040807, 1334–1438), amplicon = 105 bp; TRPM5 (XM_344979, 2645–2745), amplicon = 101 bp; TRPM6 (XM_219747, 3542–3653), amplicon = 110 bp; TRPM7 homologue (NW_047658, 4526690–4526840), amplicon = 151 bp; TRPM8 (NM_134371, 1846–1951), amplicon = 106 bp; glyceraldehyde-3-phosphate dehydrogenase (GAPDH, NM_017008, 714–817), amplicon = 104 bp.

For PCR analysis of the full coding regions of TRPC2, TRPC3 and TRPC5 (data shown in Fig. 10), a series of primers were designed for each channel. These are summarized in Table 1. Amplified products were separated on 1% agarose gels, and recovered from gel fragments using Geneclean II (Bio 101, La Jolla, CA, USA). Purified DNA fragments were identified by DNA sequencing.

Statistics

Summary data for RT-PCR are presented as means ± S.E.M. The reproducibility of the RT-PCR measurements were evaluated using an analysis of variance (ANOVA) comparing repeat runs of samples. Mean values generated at individual time points were compared by Student's *t* test. Summary data for electrophysiological experiments are presented as means ± S.E.M. Data were analysed using either the paired Student's *t* test or an ANOVA with Dunnett's multiple comparisons procedure. In all instances, $P < 0.05$ was considered significant.

Results

An initial goal of this study of CNP effects on the cardiac fibroblast was to determine whether $I_{Ca(L)}$ is modulated, since this is now known to be the case in the cardiac myocyte (Rose *et al.* 2003, 2004). However, the same voltage-clamp protocol that we used previously to measure

Table 1. PCR primers used to detect expression of full coding regions for TRPC2, TRPC3 and TRPC5 transcripts in acutely isolated rat ventricular fibroblasts

Clones	Primer sequence*	Primer site	Product length (bp)	GenBank accession no.
TRPC2	(+) 5′-ACAGAAGTGGGTGCAGCC-3′	35–52	635	NM_022638
	(–) 5′-GCGACATCCATCGTTGTTGA-3′	650–669		CDS (53–2710)
	(+) 5′-TATTGCTCGGCCCCACCCAG-3′	568–587	1067	
	(–) 5′-GCAGAATATACGCCAATCGGGTGA-3′	1611–1634		
	(+) 5′-GTGCTCTTTGCTGTCACGA-3′	1580–1598	960	
	(–) 5′-CACAATCCCAGGCATCGTC-3′	2521–2539		
	(+) 5′-CAGCATCCTCAGTCGGTACATCAC-3′	2437–2460	452	
	(–) 5′-TTAGGGGAGTGAAGGAAGGGATCT-3′	2875–2898		
TRPC3	(+) 5′-TCAGGCGGGCAGTCCACATGAT-3′	46–67	601	NM_021771
	(–) 5′-GCCCGTGTCTCTCCAGGGGTTC-3′	625–646		CDS (79–2289)
	(+) 5′-TGGAACCCCTGGAGAGACACGG-3′	623–644	801	
	(–) 5′-CGTTTGCAGGGAGAATGTACGCGA-3′	1400–1423		
	(+) 5′-AGAGATAAATGGCTTCCTTCTGAC-3′	1318–1341	982	
	(–) 5′-TGTGGCTCCCTCATTCACACCT-3′	2278–2299		
TRPC5	(+) 5′-AGTAAGGCTGTCGCACCACGC-3′	235–255	728	NM_080898
	(–) 5′-TTGATAAGGCGATGAGCGAAGGGC-3′	945–968		CDS (332–3256)
	(+) 5′-CCCTTCGCTCATCGCCTTATCA-3′	946–967	668	
	(–) 5′-TGAATCCACCATCCCACATTTCCT-3′	1590–1613		
	(+) 5′-GAAATGTGGGATGGTGGATTC-3′	1592–1612	729	
	(–) 5′-GATGTTGAAAGGAGGTGGTAAG-3′	2299–2320		
	(+) 5′-TCATCCCCAGCCCCAAATCAT-3′	2319–2339	1038	
	(–) 5′-TTAGAGCCGAGTTGTAACTT-3′	3337–3356		
GAPDH	(+) 5′-GGGGCCAAAAGGGTCATCATCTC-3′	1186–1208	549	AF106860
	(–) 5′-AGCATCAAAGGTGGAAGAATGGGA-3′	1711–1734		

*(+), Sense; (–), antisense.

CNP effects on $I_{Ca(L)}$ in cardiac myocytes (Rose *et al.* 2004) failed to identify voltage-gated inward currents in these acutely isolated fibroblasts. Specifically, there was no evidence for the presence of a Na^+ current or $I_{Ca(L)}$ in these cells (data not shown). As expected from our previous work (Chilton *et al.* 2005; Shibukawa *et al.* 2005) small K^+ currents could be measured when using superfusate and pipette solutions containing normal concentrations of K^+.

When slow voltage ramps (–100 to +100 mV over 1 s) were applied to ventricular fibroblasts from a holding potential of 0 mV, with all internal and external K^+ replaced by Cs^+ and TEA (see Methods), small inward and outward current changes were observed. Monitoring these currents in the absence of any pharmacological agonists revealed that a small weakly outwardly rectifying current with an apparent reversal potential near 0 mV was expressed in these fibroblasts (see Fig. 1 for representative examples, and summary data for the current properties in steady-state 'control' conditions). On average, the maximum inward and outward current densities in the absence of any pharmacological compounds, measured at –100 and +100 mV, were -5.80 ± 0.8 and 7.68 ± 1.4 pA pF^{-1} (see black bars in Fig. 1*C*, 1*F* and 1*I* for steady-state 'control' current densities).

The ion permeation properties of this current (activated using voltage ramps) were examined in detail and these results are summarized in Fig. 1. To determine if the current was a chloride current, NaCl was replaced with $NaCH_3SO_3$, resulting in a low external Cl^- concentration. Representative current–voltage (*I–V*) curves and time-course data are presented in Fig. 1*A* and *B*, respectively. On average, there was no significant effect of lowering the external Cl^- concentration (Fig. 1*C*), indicating that the current is not a Cl^- current. The next set of experiments measured the effect of replacing external NaCl with NMDG-Cl. As illustrated in the representative *I–V* curves (Fig. 1*D*) and time-course data (Fig. 1*E*), removing external Na^+ markedly decreased inward currents (at negative potentials) without affecting outward currents. This effect was reversible upon return to normal external Na^+ concentration. On average, maximum inward current was decreased from -3.9 ± 1.2 to -1.2 ± 0.9 pA pF^{-1} (Fig. 1*F*), indicating that the current response is primarily due to inward Na^+ movement at negative membrane potentials. The extracellular solution in which Na^+ was replaced with $NMDG^+$ still contained Ca^{2+} and Mg^{2+}, which was likely to account for the remaining inward current. Finally, the effects of removing external Ca^{2+} and Mg^{2+} were evaluated. This manoeuvre

consistently increased inward and outward currents and resulted in a more linear *I–V* curve (Fig. 1*G* and *H*), an effect that was completely reversible upon return to normal divalent ion concentrations (Fig. 1*H*). On average, maximum inward and outward currents in basal conditions were -5.4 ± 0.5 and 7.1 ± 1.1 pA pF^{-1}. These values were significantly increased to -7.9 ± 0.8 and 10.0 ± 1.3 pA pF^{-1} upon removal of external Ca^{2+} and Mg^{2+} (Fig. 1*I*). This effect of divalent cation removal suggests that divalent cations can block monovalent cation permeation in a voltage-dependent manner. This phenomenon may be responsible for the outward rectification properties of this current. Similar results have been reported for other non-selective cation ion channels (Prakriya & Lewis, 2002). Taken together, the data presented in Fig. 1 demonstrate that the current measured with voltage ramps in cardiac fibroblasts has the properties of a non-selective cation conductance (NSCC).

Effects of CNP on the NSCC in cardiac fibroblasts

Figure 2 illustrates the effects of CNP and the NPR-C selective agonist cANF on the NSCC identified in rat cardiac fibroblasts. Application of CNP (2×10^{-8} M) consistently resulted in the strong activation of the NSCC. The I-V relation continued to show weak outward rectification and an apparent reversal potential of approximately 0 mV in the presence of the agonist peptide (Fig. 2*A*). The time course of this effect of CNP is presented in Fig. 2*B*. Superfusion with Tyrode solution containing CNP resulted in a slow increase in peak inward and outward currents. This effect reached a steady state in approximately 300 s at 22°C. Washout of CNP (not shown) was typically very slow, as we have observed in our studies of CNP effects on $I_{Ca(L)}$ in cardiac myocytes (Rose *et al.* 2003, 2004). However, when washout of CNP was continued for 15 min or longer, a partial return to control current levels was observed. On average, peak inward and outward currents were -3.8 ± 0.8 and 5.3 ± 0.2 pA pF^{-1}, respectively, in steady-state control conditions. Following the application of CNP, these values increased to -48.7 ± 7.2 and 128.8 ± 16.3 pA pF^{-1} (Fig. 2*G*).

This same experimental protocol was repeated after cANF (2×10^{-8} M), which is a selective agonist for the NPR-C receptor subtype, was added to the superfusate. cANF does not bind to the NPR-A or NPR-B receptors, hence it cannot modulate intracellular cGMP levels (Anand-Srivastava *et al.* 1990). Rather, cANF binds to NPR-C and activates an inhibitory G protein, G_i (Pagano & Anand-Srivastava, 2001; Zhou & Murthy, 2003). Representative *I–V* curves (Fig. 2*C*) and time-course data (Fig. 2*D*) demonstrate that the effects of cANF on the NSCC were indistinguishable from the effect of CNP. On average, peak inward and outward currents were -5.1 ± 0.7 and 5.6 ± 1.6 pA pF^{-1} in control conditions. Following the application of cANF, these values increased to -42.0 ± 8.1 and 139.1 ± 14.3 pA pF^{-1}, respectively (Fig. 2*G*). There was no significant difference between the effects of CNP and the NPR-C agonist cANF on isolated cardiac fibroblasts. These findings suggest that this CNP effect is mediated by the NPR-C receptor. The responses of the CNP/cANF-activated NSCC to external Cl^- replacement, external Na^+ replacement and external divalent cation removal were very similar to the responses shown in basal conditions in Fig. 1 (data not shown). This indicates that the outward rectification of the cANF-activated NSCC is due to a voltage-dependent block by divalent cations, as described for other non-selective currents (Nilius *et al.* 2000; Prakriya & Lewis, 2002).

Because NPR-C is known to signal via an inhibitory G_i protein, we tested the effects of carbachol (CCh; 1×10^{-5} M) (which also activates G_i proteins via muscarinic receptors) on the fibroblast NSCC. Representative *I–V* curves (Fig. 2*E*) and time-course data (Fig. 2*F*) demonstrated that CCh was equally as effective as CNP or cANF in its ability to increase the fibroblast NSCC. On average, peak inward and outward currents were -5.0 ± 1.2 and 4.5 ± 1.8 pA pF^{-1} in control conditions, and -32.8 ± 10.9 and 92.3 ± 12.1 pA pF^{-1} following application of CCh (Fig. 2*G*). The effects of CNP, cANF and CCh on the NSCC in rat cardiac fibroblasts were not significantly different ($P > 0.05$).

Role of G_i in the activation of the NSCC by CNP and CCh

NPR-C-mediated natriuretic peptide effects, as well as the effects of CCh, are known to involve the activation of inhibitory G_i proteins (Wickman & Clapham, 1995; Anand-Srivastava *et al.* 1996). To confirm that this was the case in the activation of a NSCC in rat cardiac fibroblasts, suspensions of fibroblasts were pre-treated with pertussis toxin (PTX; 0.5 μg ml^{-1}) for a minimum of 3 h at 37°C in order to inactivate $G_{i/o}$ proteins. Following PTX treatment, fibroblasts were superfused normally and treated with either cANF (to activate NPR-C) or CCh at the same concentrations as used previously. Representative *I–V* curves and time-course data for cANF treatment are shown in Fig. 3*A* and *B*, respectively. In these conditions the ability of cANF to activate the NSCC was abolished. Normally, cANF increased the NSCC within approximately 300 s (see Fig. 2); however, in the presence of PTX, no effects of cANF were observed over 600 s of recording. Summary data (Fig. 3*C*) demonstrate that pre-treatment with PTX completely blocks the ability of cANF and CCh to activate the NSCC in rat cardiac fibroblasts. We noted also that fibroblasts from the same isolations that were not treated with PTX displayed normal responses to cANF and CCh (not shown).

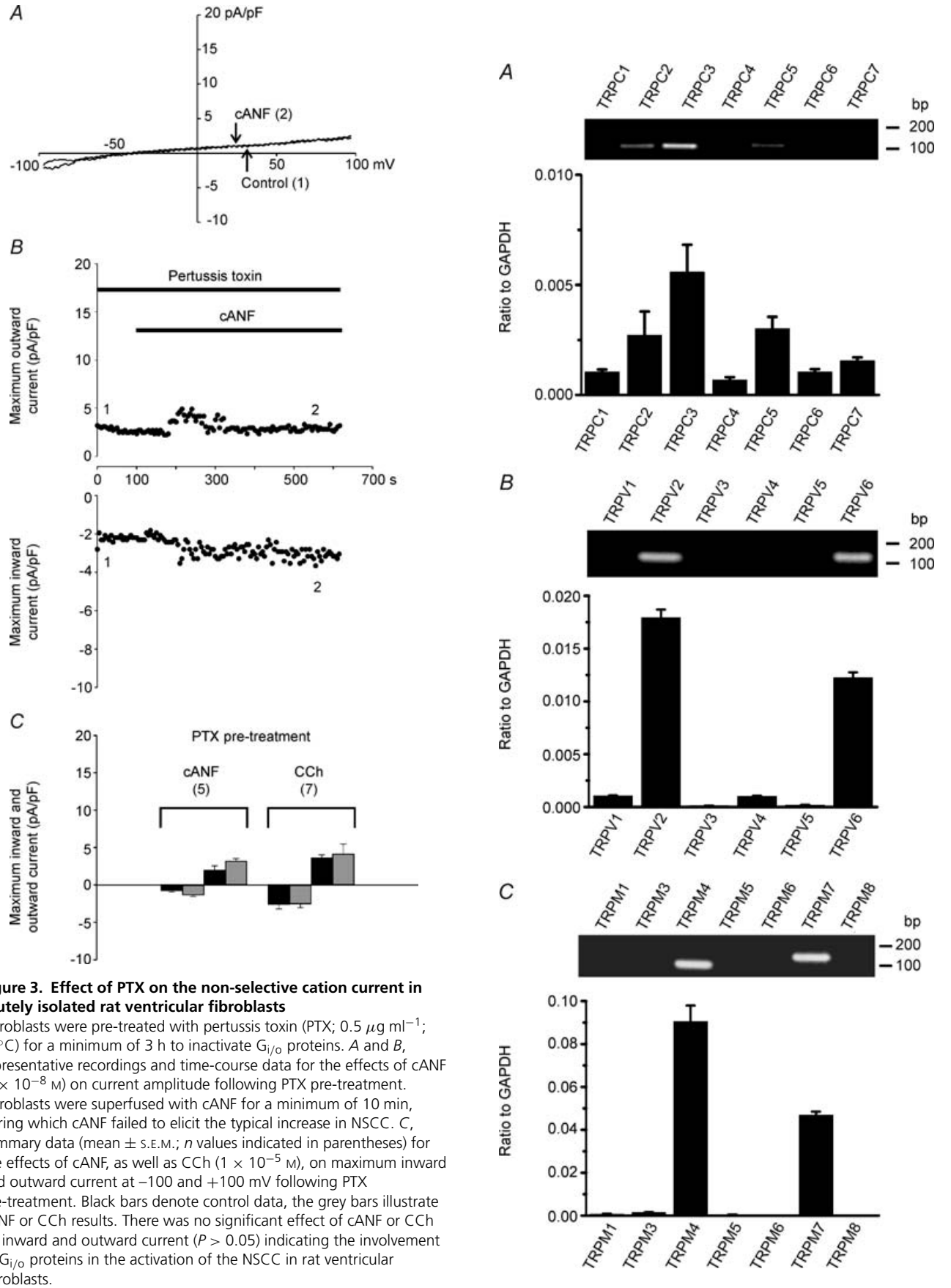

Figure 3. Effect of PTX on the non-selective cation current in acutely isolated rat ventricular fibroblasts
Fibroblasts were pre-treated with pertussis toxin (PTX; 0.5 μg ml^{-1}; 37°C) for a minimum of 3 h to inactivate $G_{i/o}$ proteins. *A* and *B*, representative recordings and time-course data for the effects of cANF (2×10^{-8} M) on current amplitude following PTX pre-treatment. Fibroblasts were superfused with cANF for a minimum of 10 min, during which cANF failed to elicit the typical increase in NSCC. *C*, summary data (mean ± S.E.M.; *n* values indicated in parentheses) for the effects of cANF, as well as CCh (1×10^{-5} M), on maximum inward and outward current at −100 and +100 mV following PTX pre-treatment. Black bars denote control data, the grey bars illustrate cANF or CCh results. There was no significant effect of cANF or CCh on inward and outward current ($P > 0.05$) indicating the involvement of $G_{i/o}$ proteins in the activation of the NSCC in rat ventricular fibroblasts.

Expression of TRP channels in cardiac fibroblasts

Numerous members of the TRP family of ion channels are known to be non-selective in terms of their ion permeation properties (Clapham *et al.* 2001; Clapham, 2003). Because of this, we hypothesized that one or more TRP channels could be responsible for the NSCC in rat cardiac fibroblasts. RT-PCR was used to study the expression of TRP channel transcripts in these acutely isolated cardiac fibroblasts. As described in Methods, RNA was isolated from rat cardiac fibroblasts and probed using specific primers developed against rat TRP channel genes. RT-PCR data depicting ion channel transcripts from the TRPC (Fig. 4*A*), TRPV (Fig. 4*B*) and TRPM (Fig. 4*C*) subfamilies are presented. Note that mRNA from several TRP channels in each subfamily is expressed. In particular, TRPC2, TRPC3, TRPC5, TRPV2, TRPV6, TRPM4 and TRPM7 consistently showed significant levels of expression in acutely isolated cardiac fibroblasts.

Pharmacological inhibition of the cANF-activated NSCC

Figure 5 demonstrates the effects of three potent, but non-selective, compounds on the cANF-activated NSCC. In this study, Gd^{3+} (1×10^{-5} M), SKF 96365 (5×10^{-5} M) and 2-aminoethoxydiphenyl borate (2-APB; 1×10^{-4} M), were tested. Each of these compounds has been shown to block currents carried by a number of TRP channels (Merritt *et al.* 1990; Halaszovich *et al.* 2000; Ma *et al.* 2000, 2001; Trebak *et al.* 2002; Prakriya & Lewis, 2002, 2003; Hunton *et al.* 2004). Representative current recordings and the time-course data for the effects of cANF (used to selectively activate NPR-C) and subsequent application of Gd^{3+} (Fig. 5*A* and *B*), SKF 96363 (Fig. 5*C* and *D*) and 2-APB (Fig. 5*E* and *F*) illustrate that each compound can potently inhibit the cANF-activated NSCC in cardiac fibroblasts. Summary data are presented in Fig. 9. On average, Gd^{3+} significantly inhibited the cANF-activated current. This effect averaged from -52.5 ± 10.8 and 98.9 ± 16.1 pA pF^{-1}, in the inward and outward directions, to -16.6 ± 9.6 and 33.5 ± 15.5 pA pF^{-1}, respectively. SKF 96365 inhibited the inward and outward components of the cANF-activated current in ventricular fibroblasts from -55.3 ± 8.8 and 115.0 ± 11.8 pA pF^{-1}, to -18.5 ± 5.8 and 35.5 ± 10.5 pA pF^{-1}, respectively. Additional results showed that 2-APB significantly inhibited the cANF-activated current, reducing it from -47.1 ± 10.2 and 111.0 ± 14.2 pA pF^{-1}, in the inward and outward directions to -21.8 ± 9.3 and 37.6 ± 9.6 pA pF^{-1}, respectively,

Figure 4. RT-PCR analysis of the molecular identity of transient receptor potential (TRP) channel transcripts in acutely isolated fibroblasts obtained from adult rat ventricles
Total RNA was isolated from adult rat fibroblasts (see Methods), and RT-PCR was used to assay the mRNA transcripts of ion channels from the TRPC (*A*), TRPV (*B*) and TRPM (*C*) subfamilies. PCR products were generated from rat gene specific primers. A 100 bp molecular mass marker was used to estimate the size of the amplicon. PCR products were sequenced to confirm their identity. Summary data are means ± S.E.M.

Voltage-dependent properties of the cANF-activated NSCC

Although initially not appreciated, it is now becoming clear that many TRP channels have time- and voltage-dependent activation properties that are responsible for the shape of the *I–V* curves of these currents (Nilius *et al.* 2005). In many instances, it is an intrinsic voltage dependence that is responsible for the outward rectification properties of TRP channels (Nilius *et al.* 2003; Voets *et al.* 2004; Grimm *et al.* 2005), while in other cases a voltage-dependent block by divalent cations causes rectification of the *I–V* curve (Nilius *et al.* 2000; Nadler *et al.* 2001; Prakriya & Lewis, 2002). Our next series of experiments investigated the time- and voltage-dependent properties of the cANF-activated TRP current in cardiac fibroblasts by utilizing voltage-clamp step protocols rather than voltage ramps.

Figure 6*A* illustrates a representative family of currents recorded in control conditions and following superfusion with cANF (2×10^{-8} M). Currents were recorded using 500 ms voltage clamp steps from –100 to +100 mV in 20 mV increments (see Fig. 6*A*, bottom). Note that the current changes in response to this protocol (in both control conditions and in the presence of cANF) did not show any measurable time dependence. They are essentially instantaneous. As shown in Fig. 6*B* the summary *I–V* curves obtained from voltage-clamp steps are indistinguishable from those obtained using voltage ramps. On average, peak inward and outward currents in control conditions were -8.1 ± 4.9 and 19.5 ± 9.7 pA pF^{-1}, respectively. Application of cANF significantly increased these peak current values to -57.3 ± 18.6 and 146.9 ± 38.4 pA pF^{-1} in the inward and outward directions. Note that these values are very similar to the average values for peak inward and outward currents obtained using voltage-ramp protocols (Fig. 2). As with voltage ramps, the cANF-activated NSCC shows weak outward rectification and reverses near 0 mV when studied with voltage-clamp step protocols.

To determine if the cANF-activated NSCC exhibits intrinsic voltage-dependent properties (Nilius *et al.* 2005), we used a voltage-clamp protocol consisting of a 500 ms prepulse to 100 mV followed by a series of voltage-clamp steps from –100 to +100 mV in 20 mV increments (Fig. 6*C*). The representative current change during this protocol was recorded in the presence of cANF (2×10^{-8} M) in the same cell as Fig. 6*A*. This voltage-clamp protocol did not elicit any tail currents as would be

expected if these channels showed significant time and voltage dependence. In fact, the *I–V* curve (Fig. 6*D*) remained unchanged from that in Fig. 6*B*.

Figure 6*E* illustrates the use of a voltage-clamp protocol consisting of a series of 500 ms voltage clamp steps from –100 to +100 mV in 20 mV increments followed by a 500 ms voltage-clamp step to –100 mV. This representative recording was done in the presence of cANF (2×10^{-8} M) in the same cell as Fig. 6*A* and *C*. The current response during the series of voltage-clamp steps from –100 to +100 mV and resulting *I–V* curve (Fig. 6*F*) were unchanged from those in Fig. 6*A–D*. Furthermore, there were no tail currents evident during the pulse to –100 mV. These results (Fig. 6*C–F*) demonstrate that the cANF-activated NSCC does not display intrinsic voltage sensitivity.

Role of phospholipase C in the activation of the NSCC by cANF

Although the biochemical and molecular mechanisms responsible for the activation of TRP channels are not completely understood, activation of phospholipase C (PLC) can be importantly involved, particularly for the TRPC subfamily. As such, several members of the TRPC subfamily are classified as receptor-operated channels and are linked to PLC activation (Clapham *et al.* 2001, 2003). Support for the involvement of PLC in the activation of a NSCC by CNP/NPR-C in acutely isolated cardiac fibroblasts is presented in Fig. 7. These results demonstrate the inhibitory effect of U73122 (5×10^{-6} M), a PLC antagonist (Kobrinsky *et al.* 2000; Cho *et al.* 2001),

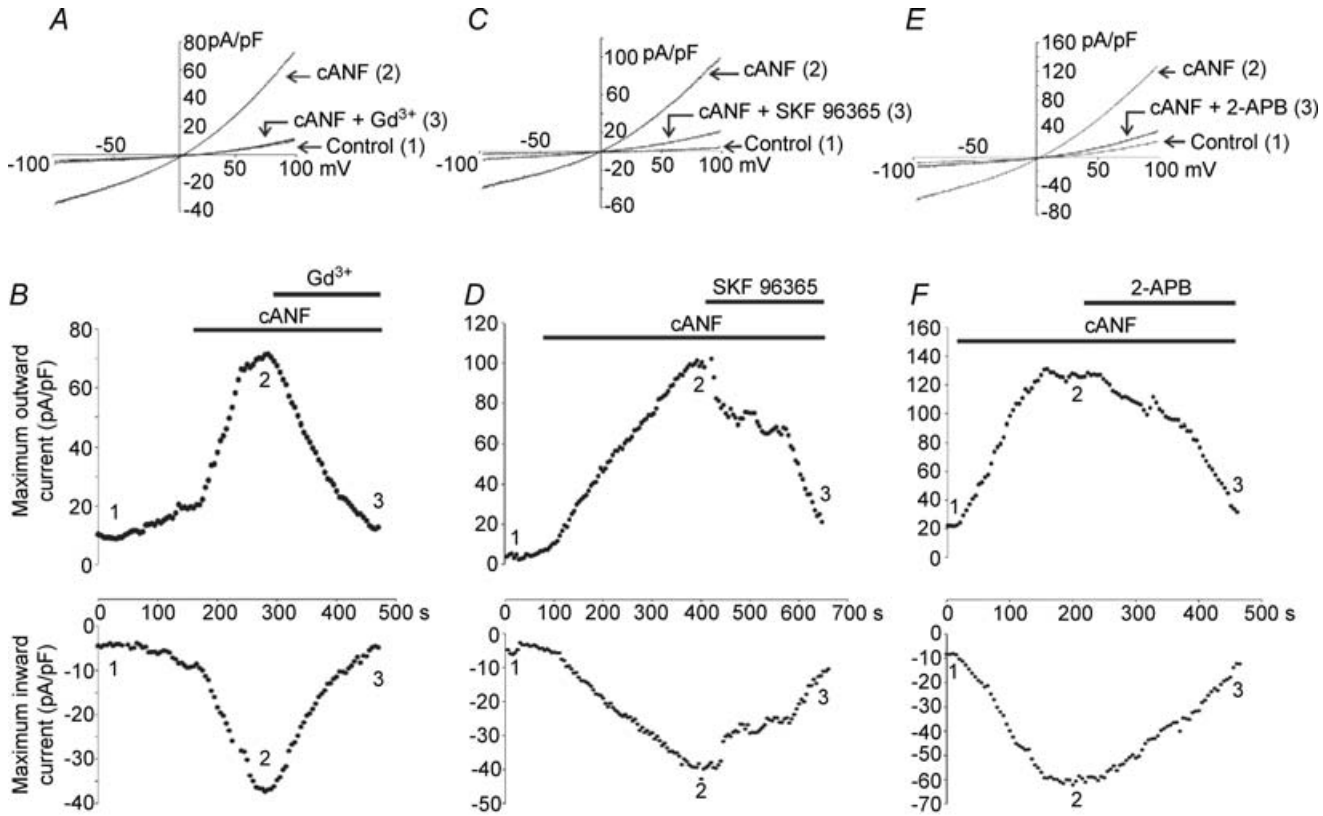

Figure 5. Effects of Gd^{3+}, SKF 96365 and 2-aminoethoxydiphenyl borate (2-APB) on the cANF-activated non-selective cation current in rat cardiac fibroblasts
Currents were elicited with a 1 s voltage ramp from –100 to +100 mV (holding potential was 0 mV). *A*, representative current changes in control conditions (1), following the application of cANF (2×10^{-8} M) (2), and during superfusion with cANF and Gd^{3+} (1×10^{-5} M) (3). *B*, time course of the effects of cANF and Gd^{3+} on inward and outward currents in the cardiac fibroblast. The representative traces correspond to the time points indicated in the time-course figure. *C*, representative current recordings in control conditions (1), following the application of cANF (2×10^{-8} M) (2), and during superfusion with cANF and SKF 96365 (5×10^{-5} M) (3). *D*, time course of the effects of cANF and SKF 96365 on inward and outward currents in the cardiac fibroblast. *E*, representative current recordings in control conditions (1), following superfusion with cANF (2×10^{-8} M) (2), and during the application of cANF and 2-APB (1×10^{-4} M) (3). *F*, time course of the effects of cANF and 2-APB on the NSCC in the cardiac fibroblast. Note that each pharmacological compound potently inhibited the NSCC activated by cANF. Data are representative of measurements made on six fibroblasts for the Gd^{3+} experiment, seven fibroblasts for the SKF 96365 experiment, and five fibroblasts for the 2-APB experiment (refer to Fig. 9 for summary data).

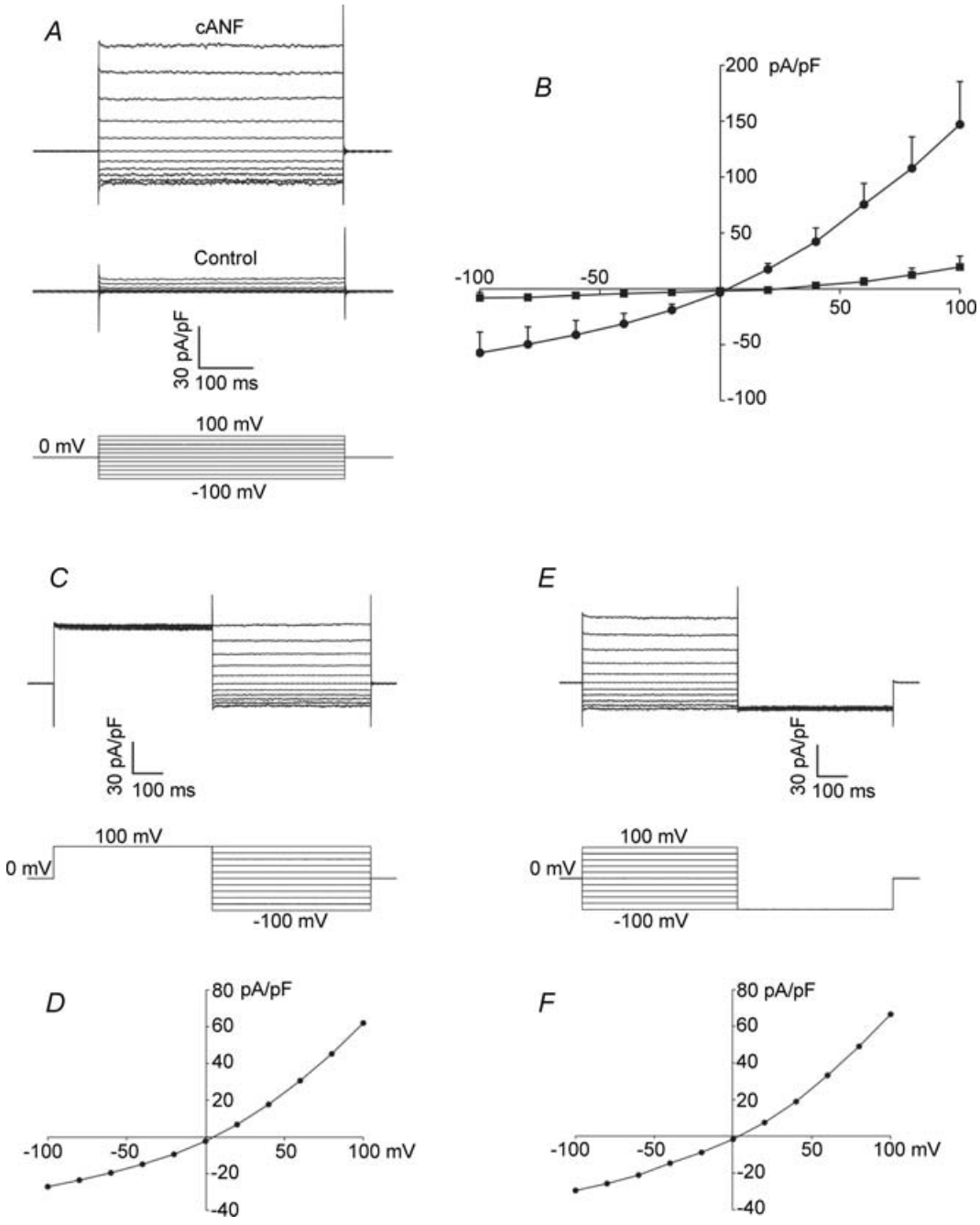

Figure 6. Properties of the cANF-activated non-selective cation current (NSCC) evaluated using rectangular voltage-clamp step protocols

A, families of currents recorded using 500 ms voltage-clamp steps from −100 to +100 mV (holding potential, 0 mV) in control conditions and following the application of cANF (2×10^{-8} M). Note that the currents show the same weak outward rectification properties as seen in response to voltage ramps. *B*, summary data illustrating the *I–V* curves in control conditions (■) and following cANF superfusion (●) obtained from voltage-step protocols as illustrated in *A*. cANF significantly increased inward and outward currents (mean ± S.E.M.; $n = 5$ fibroblasts). *C*, two-pulse protocol consisting of a prepulse to +100 mV followed by a series of voltage-clamp steps from −100 to +100 mV (in 20 mV increments) recorded in the same cell as shown in *A*. The current responses were recorded in the presence of cANF. Note that the inward and outward current densities measured during the test pulses are unchanged from those in *A*. *D*, the *I–V* curve, plotted from the voltage-clamp steps illustrated in *C*. Note that it has not significantly changed from that presented in *B*. *E*, two-pulse protocol consisting of a family of voltage-clamp steps from −100 to +100 mV followed by a step to −100 mV recorded in the same fibroblast. The sample data shown were recorded in the presence of cANF. *F*, representative *I–V* curve plotted from the family of voltage-clamp steps in *E*. Note the absence of tail currents in *C* and *E*.

on the cANF-activated NSCC. The representative traces and time-course data are illustrated in Fig. 7*A* and *B*. On average, the maximum cANF-activated NSCC was significantly reduced by U73122 from -59.0 ± 16.1 and 129.6 ± 28.7 pA pF^{-1} in the inward and outward directions to -20.6 ± 6.9 and 44.6 ± 12.7 pA pF^{-1} respectively (see summary data in Fig. 9). As a control experiment for the effect of U73122 on the cANF-activated NSCC, we studied the effects of U73343 (5×10^{-6} M). This compound is a non-functional analogue of U73122 that has no effect on PLC activity (Bian *et al.* 1998). Representative current recordings and time course data are presented in Fig. 7*C* and *D*. These results demonstrate that U73343 has no effect on the NSCC activated by cANF (see also summary data in Fig. 9).

NPR-C receptors are known to activate the β isoform of PLC, following receptor-activated dissociation of the $\beta\gamma$ subunit of the G protein (Murthy & Makhlouf, 1999; Murthy *et al.* 2000; Zhou & Murthy, 2003). Our results support the hypothesis that PLC is an important signalling molecule in the NPR-C-mediated activation of a NSCC in the cardiac fibroblast.

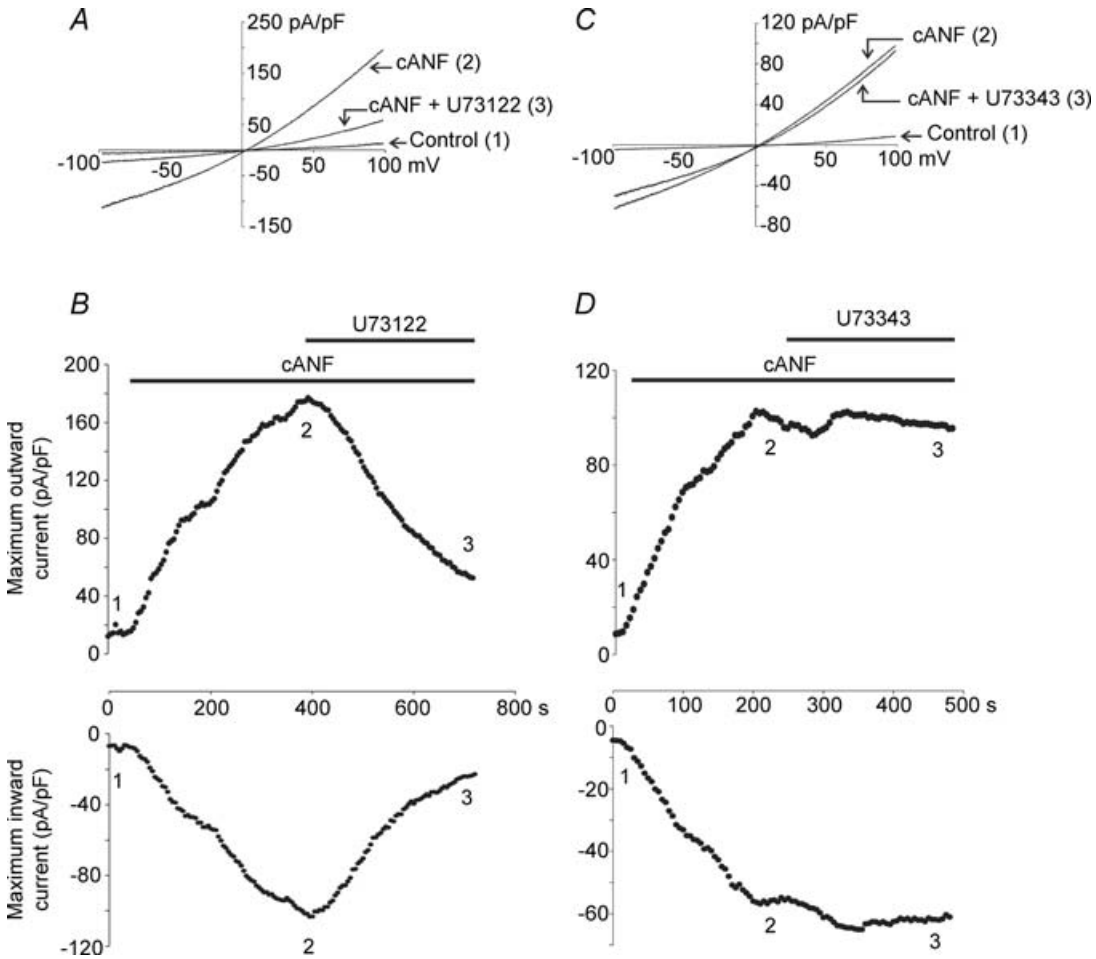

Figure 7. Effect of the phospholipase C (PLC) antagonist U73122, and its inactive analogue U73343, on the cANF-activated non-selective cation current in rat cardiac fibroblasts
Currents were studied using 1 s voltage ramps from −100 to +100 mV (holding potential was 0 mV). *A*, representative current recordings in control conditions (1), following superfusion with cANF (2×10^{-8} M) (2), and during the application of cANF and U73122 (5×10^{-6} M) (3). *B*, time course of the effects of cANF and U73122. Representative traces correspond to the time points indicated in time-course figure. *C*, representative current recordings in control conditions (1), following superfusion with cANF (2×10^{-8} M) (2), and during application of cANF in combination with U73343 (5×10^{-6} M) (3). Note that U73343 is a non-functional analogue of U73122. It has no effect on PLC activity. *D*, time course of the effects of cANF and U73343. These data are representative of measurements made on five fibroblasts for the U73122 experiment, and six fibroblasts for the U73343 experiment (refer to Fig. 9 for summary data). U73122 significantly inhibited the cANF-activated non-selective cation current, while U73343 had no significant effect.

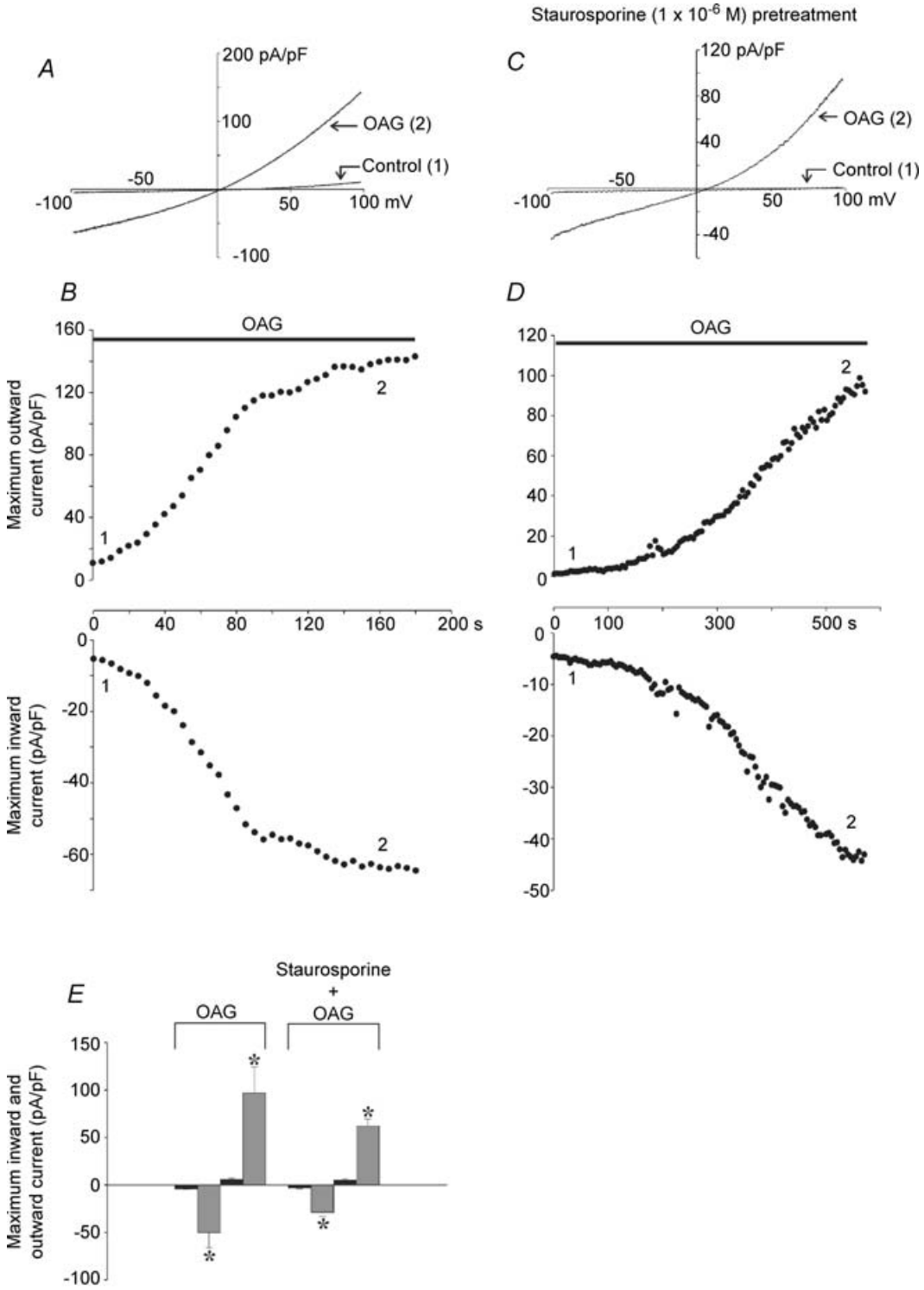

Figure 8. Effects of intracellular application of OAG on isolated rat cardiac fibroblasts
OAG (1-oleoyl-2-acetyl-*sn*-glycerol), which is an analogue of diacylglycerol, was included in the recording pipette at a concentration of 1×10^{-4} M. It entered the cell by diffusion under conventional whole-cell recording conditions. Currents were studied using a voltage ramp from –100 to +100 mV from a holding potential of 0 mV. *A*, representative current recordings under control conditions (1), and after OAG has entered the fibroblast (2). *B*, time course of the effects of OAG on cardiac fibroblasts. Representative traces correspond to the time points indicated in the time-course figure. Because OAG was in the recording pipette, it entered the fibroblasts upon establishment of the whole-cell recording condition at time 0 s. *C*, representative current recordings under control conditions (1), and after OAG had entered the fibroblast (2) following pretreatment with staurosporine

Involvement of TRPC cation channels in the activation of the NSCC

Our data demonstrates a voltage-dependent block by divalent cations, as opposed to an intrinsic voltage dependence (Fig. 6). This finding and the involvement of PLC (Fig. 7) are suggestive of a possible involvement of one or more TRPC channels in the activation of the NSCC by cANF. PCR analysis (Fig. 4) detected the expression of TRPC2, TRPC3 and TRPC5 transcripts (TRPC3 was most highly expressed) in acutely isolated cardiac fibroblasts. TRPC2 and TRPC3 are known to be directly activated by DAG (Hofmann *et al.* 1999; Lucas *et al.* 2003), which is a product of phosphatidylinositol 4,5-bisphosphate (PIP_2) hydrolysis catalysed by PLC. Based on this rationale, we tested the ability of 1-oleoyl-2-acetyl-*sn*-glycerol (OAG), which is a functional analogue of DAG, to mimic the effects of CNP and cANF on acutely isolated cardiac fibroblasts. Representative current recordings and time-course data are shown in Fig. 8*A* and *B*. OAG was included in the recording pipette at a concentration of 1×10^{-4} M so that it could enter the cell by diffusion under whole-cell recording conditions. Immediately upon rupture of the cell membrane, OAG entered the fibroblast and activated a current response that was indistinguishable from that of CNP or cANF. On average, OAG increased maximum inward and outward currents from -4.4 ± 0.6 and 8.0 ± 1.5 pA pF^{-1} in control conditions (at time 0 s) to -50.3 ± 15.6 and 97.7 ± 27.2 pA pF^{-1} (Fig. 8*E*).

Since the activation of certain TRPC channels by DAG occurs independently of PKC, we repeated the OAG experiment in fibroblasts that had been pre-treated with staurosporine (1×10^{-6} M) for a minimum of 30 min to block PKC activity (Hofmann *et al.* 1999). Representative *I–V* curves (Fig. 8*C*) and time-course data (Fig. 8*D*) show that OAG still activated the NSCC, even in the absence of PKC activity. On average, OAG (following staurosporine pre-treatment) increased maximum inward and outward currents from -3.2 ± 0.7 and 5.3 ± 1.2 pA pF^{-1} in control conditions (time, 0 min) to -28.9 ± 4.3 and 62.3 ± 7.3 (Fig. 8*E*). Although the trend was for the effect of OAG to be smaller in the presence of staurosporine (Fig. 8*E*), this difference was not statistically significant ($P > 0.05$). This result is strongly indicative of the cANF-activated NSCC being carried at least in part by one of the DAG-activated TRPC channels, such as TRPC2 or TRPC3 (see Discussion).

A summary of the effects of selected pharmacological compounds on the cANF-activated non-selective cation current in acutely isolated rat ventricular fibroblasts is presented in Fig. 9.

To provide further support for the expression of TRPC channels in cardiac fibroblasts, we performed additional molecular analysis in which full-length transcripts of the three TRPC channels detected in our initial screen (shown in Fig. 4) were amplified by PCR. Specifically, three or four pairs of PCR primers were designed to cover the full coding regions of TRPC2, TRPC3 and TRPC5 in rat cardiac fibroblasts. For all PCR primers examined, the PCR fragments with the predicted lengths (summarized in Table 1 in Methods) were observed in rat cardiac fibroblasts (Fig. 10). These results confirm that rat ventricular express full-length transcripts for TRPC2, TRPC3, and TRPC5. The smaller transcripts amplified by some primer pairs in Fig. 10 were confirmed to have no similarity to TRPC channel transcripts.

Discussion

Involvement of TRP channels in the cANF-activated NSCC

Our findings provide evidence that cardiac fibroblasts express a weakly outwardly rectifying NSCC that reverses at approximately 0 mV. These results also demonstrate that CNP, acting via the NPR-C receptor and the activation of G_i proteins, significantly potentiates this current. The cANF-activated NSCC is potently inhibited by several well-characterized, albeit non-selective, compounds, including Gd^{3+}, SKF 96365 and 2-APB. The RT-PCR data in Figs 4 and 10 demonstrate that several TRP channel transcripts are expressed in these cardiac fibroblasts. The additional experimental results presented in Figs 5–8 support the conclusion that the NSCC current activated by CNP and cANF is carried at least in part by channels that are within the TRPC subfamily, particularly the DAG-activated TRPC channels. This conclusion is based on (i) the cANF-activated TRP current being blocked by PTX and the PLC antagonist U73122 (Clapham *et al.* 2001); (ii) activation of the current being mimicked by intracellular application of OAG, independently of PKC activity (Hofmann *et al.* 1999); and (iii) the

Figure 8
(1×10^{-6} M). Cells were preincubated with staurosporine for 30 min in order to block protein kinase C (PKC) activity before being voltage clamped. *D*, time course of the effects of OAG following pretreatment of fibroblasts with staurosporine. *E*, summary data (mean ± S.E.M.) showing the effects of OAG ($n = 5$ fibroblasts), and OAG following staurosporine pretreatment ($n = 7$ fibroblasts), on maximum inward and outward currents in these acutely isolated ventricular fibroblasts. Black bars denote control data, shaded bars depict results following the application of OAG. *Significant difference between control and OAG application. Note that OAG mimics the ability of cANF to activate the NSCC in cardiac fibroblasts, and that this occurs independently of PKC activity.

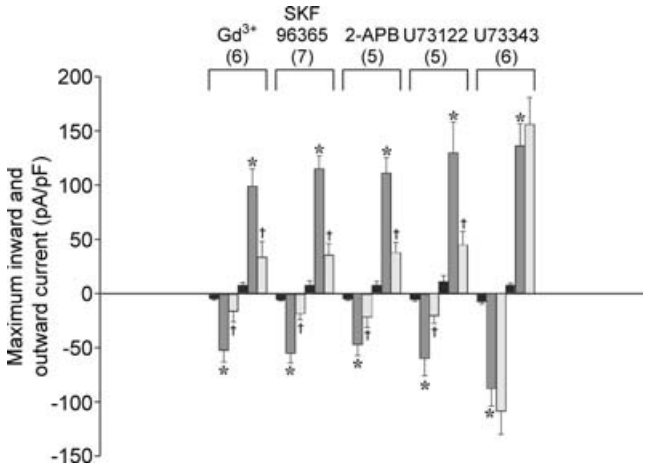

Figure 9. Summary of effects of selected pharmacological compounds on the cANF-activated NSCC in acutely isolated rat ventricular fibroblasts
In these histograms, black bars denote control data, darkly shaded bars depict results following the application of cANF, and lightly shaded bars correspond to data following the application of cANF in combination with the indicated compound. Concentrations of all drugs and chemicals are given in the previous figures. *The value in the presence of cANF is significantly different from control. †The value in the presence of cANF and the indicated compound is significantly different than in cANF alone. Data are means ± S.E.M., *n* values are indicated in parentheses.

outward rectification of the current being the result of a voltage-dependent block by divalent cations (the *I–V* curve is linearized in divalent-free external solution) rather than an intrinsic voltage dependence (Nilius *et al.* 2005). Many TRPC channels are known to be activated by G-protein-coupled receptors and the PLC pathway, and they are therefore classified as receptor-operated cation channels (Clapham *et al.* 2001; Owsianik *et al.* 2006). Furthermore, TRPC2, TRPC3, TRPC6 and TRPC7 are known to be activated directly by DAG, independently of PKC phosphorylation (Hofmann *et al.* 1999; Lucas *et al.* 2003; Zufall *et al.* 2005). This direct effect of DAG on channel activity is a defining characteristic of these TRPC channels. The finding that TRPC2 and TRPC3 mRNAs are expressed in our acutely isolated cardiac fibroblasts leads to the conclusion that TRPC2 and/or TRPC3 may be activated by CNP and the NPR-C receptor. However, it is not possible, based on our experimental data alone, to conclude that TRPC2 and/or TRPC3 are the only ion channels responsible for the activation of the NSCC by CNP/NPR-C-mediated signalling in the cardiac fibroblast. Although the *I–V* curve of the NSCC measured in this study bears significant similarities to the *I–V* curve of heterologously overexpressed TRPC3 channels (Dietrich *et al.* 2003; Lee *et al.* 2003), it remains possible that the CNP-activated NSCC is carried by heteromultimeric and/or multiple channels with properties unique from those measured in expression systems (see discussion of limitations of this study below).

The activation of a NSCC by CNP can be mimicked by application of the NPR-C agonist, cANF. This finding strongly implicates an important functional role for this receptor subtype in this electrophysiological response. Although, in general, NPR-C has been assigned the role of a 'clearance receptor' whose function is to modulate the circulating levels of natriuretic peptides available to bind to the NPR-A and NPR-B receptors (Levin *et al.* 1998), it is now known to be functionally linked to a G_i protein (Anand-Srivastava *et al.* 1996). Our data suggest that the activation of the NSCC current by CNP and the NPR-C receptor involves the activation of G_i and PLC (Figs 3 and 7). The $\beta\gamma$ subunits of G proteins are known to stimulate the β isoform of PLC (Katz *et al.* 1992; Barr *et al.* 2000). Moreover, dissociation of the heterotrimeric G_i protein specifically activated by NPR-C has been shown to lead to the stimulation of PLC by these $\beta\gamma$ subunits (Murthy & Makhlouf, 1999; Murthy *et al.* 2000; Zhou & Murthy, 2003). PLC catalyses the conversion of PIP_2 into diacylglycerol (DAG) and inositol 1,4,5-trisphosphate (IP_3). Our results also demonstrated that OAG mimicked the effects of CNP and cANF on the NSCC (Fig. 8). Indeed, DAG is able to directly activate both TRPC2 and TRPC3 channels independently of PKC (Hofmann *et al.* 1999; Lucas *et al.* 2003). In summary, our findings support the hypothesis that CNP binds to the NPR-C receptor, activates a G_i protein, and the resulting liberation of $\beta\gamma$ subunits stimulates the conversion of PIP_2 to DAG and IP_3 by PLCβ. DAG would then be able to directly activate TRPC cation channels in cardiac fibroblasts.

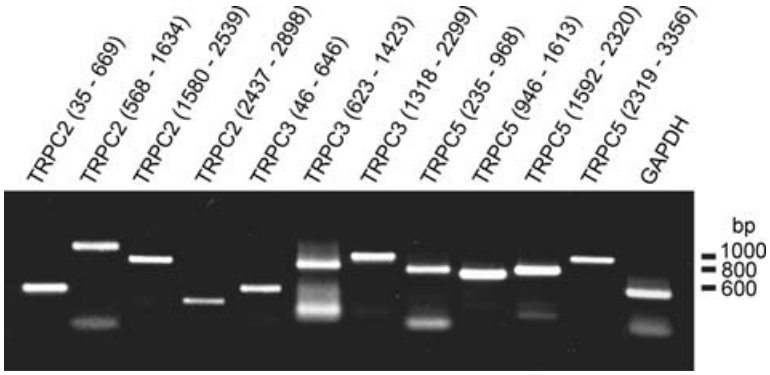

Figure 10. RT-PCR detection of mRNA transcripts covering the full coding regions of TRPC2, TRPC3 and TRPC5 in rat cardiac fibroblasts
PCR products were generated through the use of gene-specific primers for TRPC2 (lanes 1–4 from the left), TRPC3 (lanes 5–7), and TRPC5 (lanes 8–11). A molecular mass marker was used to estimate the size of the amplicon. RT-PCR was also performed in the presence of glyceraldehyde-3-phosphate dehydrogenase (GAPDH), an internal standard (lane 12). Similar results were obtained from four independent cardiac fibroblast cDNA preparations. Refer to Table 1 for primer details.

In humans, the TRPC2 gene is thought to be encoded by a pseudogene. In rodents, TRPC2 has been found to be highly localized to the vomeronasal organ where it functions in pheromone sensing and regulation of social behaviour (Zufall *et al.* 2005). If TRPC2 is in fact activated by CNP and NPR-C in cardiac fibroblasts, this would represent an important, but previously unrecognized, role for this ion channel in the fibroblast population of the heart. TRPC3 is known to be expressed at significant levels in cardiac myocytes and smooth muscle cells. This has led to speculation that this channel may be a candidate for a receptor-activated non-selective cation conductance in these locations (Clapham, 2003). As TRPC3 was the most highly expressed TRPC channel in acutely isolated cardiac fibroblasts, this channel may be a significant target of CNP/NPR-C signalling. Our molecular analysis (Figs 4 and 10) also detected the expression of TRPC5 transcript. TRPC5 is known to be activated by pertussis toxin sensitive G proteins and the PLC pathway (Xu *et al.* 2006); therefore, TRPC5 could also be involved in the CNP/NPR-C response. The *I–V* curve of TRPC5, as measured in overexpression systems, shows rectification properties that differ significantly from the *I–V* curves we have measured in cardiac fibroblasts, although this can change when the channel coassembles with other TRPC proteins (Strubing *et al.* 2003; Xu *et al.* 2006). Further molecular work will be required to define the precise role of different TRPC channels in the CNP response in cardiac fibroblasts.

In addition to TRPC2, TRPC3 and TRPC5, RT-PCR data revealed the expression of several other TRP channel transcripts in the cardiac fibroblast (Fig. 4). In particular, mRNA for TRPV2, TRPV6, TRPM4 and TRPM8 all showed significant expression levels. However, based on their pharmacological and electrophysiological properties these channels do not appear to be involved in the response to CNP in ventricular fibroblasts. TRPV2 is activated by 2-APB (Hu *et al.* 2004), whereas the CNP-activated TRP current is blocked by this compound. 2-APB is known to function as a consistent blocker of channels in the TRPC subfamily, including TRPC3 (Ma *et al.* 2000, 2001). TRPV6 is one of the most Ca^{2+}-selective TRP channels and has a strongly inwardly rectifying *I–V* curve (Bodding, 2005). These properties are very different from the current activated by CNP and cANF in ventricular fibroblasts. TRPM4 is activated by intracellular Ca^{2+}, is permeable only to Na^{+}, and shows intrinsic voltage dependence (Nilius *et al.* 2003; Ullrich *et al.* 2005). Our pipette solution contained 0.1 mM $CaCl_2$ and 10 mM EGTA, making the free intracellular Ca^{2+} nominally 0 mM. Under these recording conditions, TRPM4 would not be activated. Finally, TRPM7 shows very strong outward rectification, is inactivated by hydrolysis of PIP_2, and is strongly inhibited by carbachol via the activation of muscarinic receptors (Runnels *et al.* 2002). In contrast, the NSCC activated by CNP shows weak outward rectification properties, is directly activated by DAG (presumably following the hydrolysis of PIP_2 by PLC), and is increased by carbachol following muscarinic receptor activation. It remains to be determined how these other TRP channels that were detected affect the physiology of the cardiac fibroblast and under what conditions they are modulated.

It is important to note that the present study did not investigate the possible contributions of the α_i subunit of the G protein activated by NPR-C to the electrophysiological effects of CNP on the cardiac fibroblast. NPR-C is known to negatively regulate adenylyl cyclase activity and decrease cAMP via the α subunit of G_i (Pagano & Anand-Srivastava, 2001; Zhou & Murthy, 2003). Furthermore, other studies have identified a cAMP-dependent regulation of certain TRP channels, such as TRPM7 (Takezawa *et al.* 2004). Whether a similar pattern of regulation is occurring in the cardiac fibroblast via NPR-C effects on G_i activity remains to be investigated.

We note that in our experiments the effects of CNP were mimicked by CCh (Fig. 2). A previous study showed that the effects of muscarinic agonists were minimal in cultured rat cardiac fibroblasts (Meszaros *et al.* 2000); however, the role of muscarinic acetylcholine (ACH) receptors has not been studied in acutely isolated cardiac fibroblasts. Our data, which demonstrate a potent effect of CCh that is completely abolished by pertussis toxin, strongly indicate the expression of functional muscarinic receptors. Understanding muscarinic receptor signalling in cardiac fibroblasts will require additional study.

Limitations of this study

The biophysical characterization of TRP channels under physiological conditions is still incomplete. Moreover, the lack of specific pharmacological tools remains a major limitation to the study of TRP channels in native tissues (Clapham *et al.* 2001; Clapham, 2003). Although our electrophysiological and PCR data support the conclusion that the CNP/NPR-C-activated NSCC may involve TRPC2, TRPC3 and/or TRPC5 there are no specific blockers for these channels. It is for these reasons that many TRP channel studies employ the use of heterologous expression systems to study channel properties. Our experiments were conducted in acutely isolated cardiac fibroblasts. The results provide novel insights into the electrophysiological effects of CNP and NPR-C in these cells. Although the data in this study clearly suggest TRPC channels are involved in the NPR-C-mediated response to CNP, definitive conclusions regarding the precise molecular identity of the TRPC channel(s) which are modulated are not possible. Future studies will endeavour to use molecular methods to confirm the conclusions drawn from the electrophysiological data presented in this study.

Consideration must also be given to the possibility that the functional characteristics of TRPC homomers measured in overexpression systems may not represent all characteristics of currents expressed in native cells. This is because it is now apparent that several members of the TRPC subfamily can form heteromultimeric channels by interacting with each other (Dietrich *et al.* 2005*a*,*b*). For example, TRPC3 is known to interact and form heteromultimeric channels with TRPC6 (Hofmann *et al.* 2002; Bandyopadhyay *et al.* 2005). There is some evidence that TRPC2 and TRPC6 can also interact (Chu *et al.* 2004), although see Hofmann *et al.* (2002). Based on this, and on the fact that our PCR data indicate that several members of the TRPC subfamily are expressed in acutely isolated cardiac fibroblasts, it seems plausible that the current activated by CNP and the NPR-C receptor is carried by heteromultimeric TRPC channels. It is also possible that other ion channels are active during the voltage ramps used in this study, which could contribute to the current changes and resulting *I–V* curves in this paper. RNA interference or dominant-negative strategies may prove useful in determining the precise contributions of specific ion channels to the CNP/NPR-C responses identified in this study (Maruyama *et al.* 2006).

A functional role for CNP in cardiac fibroblasts

Recently, we have described a novel NPR-C receptor mediated inhibition of $I_{Ca(L)}$ in cardiomyocytes (Rose *et al.* 2003, 2004). When considered in conjunction with those findings, the results of the present study raise interesting questions about the role of CNP and the NPR-C receptor in paracrine signalling in the heart. In the myocyte population of the heart, $I_{Ca(L)}$ is inhibited via NPR-C signalling. This effect is mediated by the α subunit of the G_i protein that is activated by NPR-C binding (Pagano & Anand-Srivastava, 2001; Rose *et al.* 2004). In the myocyte, G_i activation inhibits adenylyl cyclase and reduces cAMP, thus decreasing $I_{Ca(L)}$. In contrast, in the fibroblast, CNP/NPR-C signalling activates a NSCC, which may include Ca^{2+} entry through TRPC channels (Owsianik *et al.* 2006) following the activation of PLC. This effect in the fibroblast appears to be mediated by the $\beta\gamma$ subunits of the same G_i protein activated by NPR-C. Clearly, the details of these CNP/NPR-C effects on myocytes and fibroblasts, and how they may interact with each other in the heart, warrant further investigation.

Natriuretic peptides, including CNP, are upregulated and highly expressed in the setting of heart failure (Wei *et al.* 1993; Richards, 2004). Natriuretic peptides are thought to exert antifibrotic effects during heart failure by altering the secretion of collagen, matrix metalloproteinases, and various hormonal factors by the cardiac fibroblast (Horio *et al.* 2003; Kapoun *et al.* 2004; Kawakami *et al.* 2004). Furthermore, natriuretic peptide effects on cardiac fibroblast proliferation appear to involve the NPR-C receptor (Huntley *et al.* 2006). Since our results indicate that cardiac fibroblasts do not express time- and voltage-gated Na^+ or Ca^{2+} currents, TRP channels are likely to play a prominent role in regulating Na^+ and Ca^{2+} entry into these cells. It is possible that the effects of CNP and the NPR-C receptor on TRPC currents in these cells may importantly regulate the secretory properties of the fibroblast.

In summary, our findings reveal a novel role for the NPR-C receptor in the cardiac fibroblast. CNP, acting via the NPR-C receptor, G_i, PLC activity, and the production of DAG, activates a NSCC, which may involve TRPC cation channels. As TRPC channels are known to mediate an influx of cations including Ca^{2+} (Clapham, 2003) this sequence of events may be an important mechanism in the regulation of the metabolic and secretory state of the fibroblast population in the heart.

References

Allessie M, Schotten U, Verheule S & Harks E (2005). Gene therapy for repair of cardiac fibrosis: a long way to Tipperary. *Circulation* **111**, 391–393.

Anand-Srivastava MB, Sairam MR & Cantin M (1990). Ring-deleted analogs of atrial natriuretic factor inhibit adenylate cyclase/cAMP system. *Possible coupling of clearance atrial natriuretic factor receptors to adenylate cyclase/cAMP signal transduction system. J Biol Chem* **265**, 8566–8572.

Anand-Srivastava MB, Sehl PD & Lowe DG (1996). Cytoplasmic domain of natriuretic peptide receptor-C inhibits adenylyl cyclase. *Involvement of a pertussis toxin-sensitive G protein. J Biol Chem* **271**, 19324–19329.

Bandyopadhyay BC, Swaim WD, Liu X, Redman RS, Patterson RL & Ambudkar IS (2005). Apical localization of a functional TRPC3/TRPC6-Ca^{2+} signaling complex in polarized epithelial cells. *Role in apical Ca^{2+} influx. J Biol Chem* **280**, 12908–12916.

Barr AJ, Ali H, Haribabu B, Snyderman R & Smrcka AV (2000). Identification of a region at the N-terminus of phospholipase $C_{\beta 3}$ that interacts with G protein $\beta\gamma$ subunits. *Biochemistry* **39**, 1800–1806.

Baudino TA, Carver W, Giles W & Borg TK (2006). Cardiac fibroblasts: friend or foe? *Am J Physiol Heart Circ Physiol* **291**, H1015–H1026.

Bian JS, Zhang WM, Xia Q & Wong TM (1998). Phospholipase C inhibitors attenuate arrhythmias induced by κ receptor stimulation in the isolated rat heart. *J Mol Cell Cardiol* **30**, 2103–2110.

Bodding M (2005). Voltage-dependent changes of TRPV6-mediated Ca^{2+} currents. *J Biol Chem* **280**, 7022–7029.

Brilla CG & Maisch B (1994). Regulation of the structural remodeling of the myocardium: from hypertrophy to heart failure. *Eur Heart J* **15** (Suppl. D), 45–52.

Brilla CG, Maisch B, Zhou G & Weber KT (1995). Hormonal regulation of cardiac fibroblast function. *Eur Heart J* **16** (Suppl. C), 45–50.

Chilton L, Ohya S, Freed D, George E, Drobic V, Shibukawa Y, MacCannell KA, Imaizumi Y, Clark RB, Dixon IM & Giles WR (2005). K^+ currents regulate the resting membrane potential, proliferation, and contractile responses in ventricular fibroblasts and myofibroblasts. *Am J Physiol Heart Circ Physiol* **288**, H2931–H2939.

Cho H, Youm JB, Ryu SY, Earm YE & Ho WK (2001). Inhibition of acetylcholine-activated K^+ currents by U73122 is mediated by the inhibition of PIP_2 channel interaction. *Br J Pharmacol* **134**, 1066–1072.

Chu X, Tong Q, Cheung JY, Wozney J, Conrad K, Mazack V, Zhang W, Stahl R, Barber DL & Miller BA (2004). Interaction of TRPC2 and TRPC6 in erythropoietin modulation of calcium influx. *J Biol Chem* **279**, 10514–10522.

Clapham DE (2003). TRP channels as cellular sensors. *Nature* **426**, 517–524.

Clapham DE, Runnels LW & Strubing C (2001). The TRP ion channel family. *Nat Rev Neurosci* **2**, 387–396.

Dietrich A, Kalwa H, Rost BR & Gudermann T (2005*a*). The diacylgylcerol-sensitive TRPC3/6/7 subfamily of cation channels: functional characterization and physiological relevance. *Pflugers Arch* **451**, 72–80.

Dietrich A, Mederos y Schnitzler M, Emmel J, Kalwa H, Hofmann T & Gudermann T (2003). *N*-linked protein glycosylation is a major determinant for basal TRPC3 and TRPC6 channel activity. *J Biol Chem* **278**, 47842–47852.

Dietrich A, Mederos y Schnitzler M, Kalwa H, Storch U & Gudermann T (2005*b*). Functional characterization and physiological relevance of the TRPC3/6/7 subfamily of cation channels. *Naunyn Schmiedebergs Arch Pharmacol* **371**, 257–265.

Ellmers LJ, Knowles JW, Kim HS, Smithies O, Maeda N & Cameron VA (2002). Ventricular expression of natriuretic peptides in $Npr1^{-/-}$ mice with cardiac hypertrophy and fibrosis. *Am J Physiol Heart Circ Physiol* **283**, H707–H714.

Grimm C, Kraft R, Schultz G & Harteneck C (2005). Activation of the melastatin-related cation channel TRPM3 by D-erythro-sphingosine. *Mol Pharmacol* **67**, 798–805.

Halaszovich CR, Zitt C, Jungling E & Luckhoff A (2000). Inhibition of TRP3 channels by lanthanides. *Block from the cytosolic side of the plasma membrane. J Biol Chem* **275**, 37423–37428.

Hamill OP, Marty A, Neher E, Sakmann B & Sigworth FJ (1981). Improved patch-clamp techniques for high-resolution current recording from cells and cell-free membrane patches. *Pflugers Arch* **391**, 85–100.

Hofmann T, Obukhov AG, Schaefer M, Harteneck C, Gudermann T & Schultz G (1999). Direct activation of human TRPC6 and TRPC3 channels by diacylglycerol. *Nature* **397**, 259–263.

Hofmann T, Schaefer M, Schultz G & Gudermann T (2002). Subunit composition of mammalian transient receptor potential channels in living cells. *Proc Natl Acad Sci U S A* **99**, 7461–7466.

Horio T, Tokudome T, Maki T, Yoshihara F, Suga S, Nishikimi T, Kojima M, Kawano Y & Kangawa K (2003). Gene expression, secretion, and autocrine action of C-type natriuretic peptide in cultured adult rat cardiac fibroblasts. *Endocrinology* **144**, 2279–2284.

Hu HZ, Gu Q, Wang C, Colton CK, Tang J, Kinoshita-Kawada M, Lee LY, Wood JD & Zhu MX (2004). 2-aminoethoxydiphenyl borate is a common activator of TRPV1, TRPV2, and TRPV3. *J Biol Chem* **279**, 35741–35748.

Huntley BK, Sandberg SM, Noser JA, Cataliotti A, Redfield MM, Matsuda Y & Burnett JC Jr (2006). BNP-induced activation of cGMP in human cardiac fibroblasts: Interactions with fibronectin and natriuretic peptide receptors. *J Cell Physiol* **209**, 943–949.

Hunton DL, Zou L, Pang Y & Marchase RB (2004). Adult rat cardiomyocytes exhibit capacitative calcium entry. *Am J Physiol Heart Circ Physiol* **286**, H1124–H1132.

Kapoun AM, Liang F, O'Young G, Damm DL, Quon D, White RT, Munson K, Lam A, Schreiner GF & Protter AA (2004). B-type natriuretic peptide exerts broad functional opposition to transforming growth factor β in primary human cardiac fibroblasts: fibrosis, myofibroblast conversion, proliferation, and inflammation. *Circ Res* **94**, 453–461.

Katz A, Wu D & Simon MI (1992). Subunits $\beta\gamma$ of heterotrimeric G protein activate β_2 isoform of phospholipase C. *Nature* **360**, 686–689.

Kawakami R, Saito Y, Kishimoto I, Harada M, Kuwahara K, Takahashi N, Nakagawa Y, Nakanishi M, Tanimoto K, Usami S, Yasuno S, Kinoshita H, Chusho H, Tamura N, Ogawa Y & Nakao K (2004). Overexpression of brain natriuretic peptide facilitates neutrophil infiltration and cardiac matrix metalloproteinase-9 expression after acute myocardial infarction. *Circulation* **110**, 3306–3312.

Kobrinsky E, Mirshahi T, Zhang H, Jin T & Logothetis DE (2000). Receptor-mediated hydrolysis of plasma membrane messenger PIP_2 leads to K^+ current desensitization. *Nat Cell Biol* **2**, 507–514.

Lee YM, Kim BJ, Kim HJ, Yang DK, Zhu MH, Lee KP, So I & Kim KW (2003). TRPC5 as a candidate for the nonselective cation channel activated by muscarinic stimulation in murine stomach. *Am J Physiol Gastrointest Liver Physiol* **284**, G604–G616.

Levin ER, Gardner DG & Samson WK (1998). Natriuretic peptides. *N Engl J Med* **339**, 321–328.

Lucas KA, Pitari GM, Kazerounian S, Ruiz-Stewart I, Park J, Schulz S, Chepenik KP & Waldman SA (2000). Guanylyl cyclases and signaling by cyclic GMP. *Pharmacol Rev* **52**, 375–414.

Lucas P, Ukhanov K, Leinders-Zufall T & Zufall F (2003). A diacylglycerol-gated cation channel in vomeronasal neuron dendrites is impaired in TRPC2 mutant mice: mechanism of pheromone transduction. *Neuron* **40**, 551–561.

Ma HT, Patterson RL, van Rossum DB, Birnbaumer L, Mikoshiba K & Gill DL (2000). Requirement of the inositol trisphosphate receptor for activation of store-operated Ca^{2+} channels. *Science* **287**, 1647–1651.

Ma HT, Venkatachalam K, Li HS, Montell C, Kurosaki T, Patterson RL & Gill DL (2001). Assessment of the role of the inositol 1,4,5-trisphosphate receptor in the activation of transient receptor potential channels and store-operated Ca^{2+} entry channels. *J Biol Chem* **276**, 18888–18896.

Maack T (1992). Receptors of atrial natriuretic factor. *Annu Rev Physiol* **54**, 11–27.

Maruyama Y, Nakanishi Y, Walsh EJ, Wilson DP, Welsh DG & Cole WC (2006). Heteromultimeric TRPC6-TRPC7 channels contribute to arginine vasopressin-induced cation current of A7r5 vascular smooth muscle cells. *Circ Res* **98**, 1520–1527.

Merritt JE, Armstrong WP, Benham CD, Hallam TJ, Jacob R, Jaxa-Chamiec A, Leigh BK, McCarthy SA, Moores KE & Rink TJ (1990). SK&F 96365, a novel inhibitor of receptor-mediated calcium entry. *Biochem J* **271**, 515–522.

Meszaros JG, Gonzalez AM, Endo-Mochizuki Y, Villegas S, Villarreal F & Brunton LL (2000). Identification of G protein-coupled signaling pathways in cardiac fibroblasts: cross talk between G_q and G_s. *Am J PhysiolCell Physiol* **278**, C154–C162.

Muraki K, Iwata Y, Katanosaka Y, Ito T, Ohya S, Shigekawa M & Imaizumi Y (2003). TRPV2 is a component of osmotically sensitive cation channels in murine aortic myocytes. *Circ Res* **93**, 829–838.

Murthy KS & Makhlouf GM (1999). Identification of the G protein-activating domain of the natriuretic peptide clearance receptor (NPR-C). *J Biol Chem* **274**, 17587–17592.

Murthy KS, Teng BQ, Zhou H, Jin JG, Grider JR & Makhlouf GM (2000). G_{i-1}/G_{i-2}-dependent signaling by single-transmembrane natriuretic peptide clearance receptor. *Am J Physiol Gastrointest Liver Physiol* **278**, G974–G980.

Nadler MJ, Hermosura MC, Inabe K, Perraud AL, Zhu Q, Stokes AJ, Kurosaki T, Kinet JP, Penner R, Scharenberg AM & Fleig A (2001). LTRPC7 is a Mg.ATP-regulated divalent cation channel required for cell viability. *Nature* **411**, 590–595.

Nilius B, Prenen J, Droogmans G, Voets T, Vennekens R, Freichel M, Wissenbach U & Flockerzi V (2003). Voltage dependence of the Ca^{2+}-activated cation channel TRPM4. *J Biol Chem* **278**, 30813–30820.

Nilius B, Talavera K, Owsianik G, Prenen J, Droogmans G & Voets T (2005). Gating of TRP channels: a voltage connection? *J Physiol* **567**, 35–44.

Nilius B, Vennekens R, Prenen J, Hoenderop JG, Bindels RJ & Droogmans G (2000). Whole-cell and single channel monovalent cation currents through the novel rabbit epithelial Ca^{2+} channel ECaC. *J Physiol* **527**, 239–248.

Ohya S, Asakura K, Muraki K, Watanabe M & Imaizumi Y (2002). Molecular and functional characterization of ERG, KCNQ, and KCNE subtypes in rat stomach smooth muscle. *Am J Physiol Gastrointest Liver Physiol* **282**, G277–G287.

Owsianik G, Talavera K, Voets T & Nilius B (2006). Permeation and selectivity of TRP channels. *Annu Rev Physiol* **68**, 685–717.

Pagano M & Anand-Srivastava MB (2001). Cytoplasmic domain of natriuretic peptide receptor C constitutes G_i activator sequences that inhibit adenylyl cyclase activity. *J Biol Chem* **276**, 22064–22070.

Prakriya M & Lewis RS (2002). Separation and characterization of currents through store-operated CRAC channels and Mg^{2+}-inhibited cation (MIC) channels. *J Gen Physiol* **119**, 487–507.

Prakriya M & Lewis RS (2003). CRAC channels: activation, permeation, and the search for a molecular identity. *Cell Calcium* **33**, 311–321.

Richards AM (2004). The natriuretic peptides in heart failure. *Basic Res Cardiol* **99**, 94–100.

Rose RA, Lomax AE & Giles WR (2003). Inhibition of L-type Ca^{2+} current by C-type natriuretic peptide in bullfrog atrial myocytes: an NPR-C-mediated effect. *Am J Physiol Heart Circ Physiol* **285**, H2454–H2462.

Rose RA, Lomax AE, Kondo CS, Anand-Srivastava MB & Giles WR (2004). Effects of C-type natriuretic peptide on ionic currents in mouse sinoatrial node: a role for the NPR-C receptor. *Am J Physiol Heart Circ Physiol* **286**, H1970–H1977.

Runnels LW, Yue L & Clapham DE (2002). The TRPM7 channel is inactivated by PIP_2 hydrolysis. *Nat Cell Biol* **4**, 329–336.

Shibukawa Y, Chilton EL, MacCannell KA, Clark RB & Giles WR (2005). K^+ currents activated by depolarization in cardiac fibroblasts. *Biophys J* **88**, 3924–3935.

Strubing C, Krapivinsky G, Krapivinsky L & Clapham DE (2003). Formation of novel TRPC channels by complex subunit interactions in embryonic brain. *J Biol Chem* **278**, 39014–39019.

Takezawa R, Schmitz C, Demeuse P, Scharenberg AM, Penner R & Fleig A (2004). Receptor-mediated regulation of the TRPM7 channel through its endogenous protein kinase domain. *Proc Natl Acad Sci U S A* **101**, 6009–6014.

Trebak M, Bird GS, McKay RR & Putney JW Jr (2002). Comparison of human TRPC3 channels in receptor-activated and store-operated modes. *Differential sensitivity to channel blockers suggests fundamental differences in channel composition. J Biol Chem* **277**, 21617–21623.

Tsuruda T, Boerrigter G, Huntley BK, Noser JA, Cataliotti A, Costello-Boerrigter LC, Chen HH & Burnett JC Jr (2002). Brain natriuretic peptide is produced in cardiac fibroblasts and induces matrix metalloproteinases. *Circ Res* **91**, 1127–1134.

Ullrich ND, Voets T, Prenen J, Vennekens R, Talavera K, Droogmans G & Nilius B (2005). Comparison of functional properties of the Ca^{2+}-activated cation channels TRPM4 and TRPM5 from mice. *Cell Calcium* **37**, 267–278.

Voets T, Droogmans G, Wissenbach U, Janssens A, Flockerzi V & Nilius B (2004). The principle of temperature-dependent gating in cold- and heat-sensitive TRP channels. *Nature* **430**, 748–754.

Wei CM, Heublein DM, Perrella MA, Lerman A, Rodeheffer RJ, McGregor CG, Edwards WD, Schaff HV & Burnett JC Jr (1993). Natriuretic peptide system in human heart failure. *Circulation* **88**, 1004–1009.

Wickman K & Clapham DE (1995). Ion channel regulation by G proteins. *Physiol Rev* **75**, 865–885.

Xu SZ, Muraki K, Zeng F, Li J, Sukumar P, Shah S, Dedman AM, Flemming PK, McHugh D, Naylor J, Cheong A, Bateson AN, Munsch CM, Porter KE & Beech DJ (2006). A sphingosine-1-phosphate-activated calcium channel controlling vascular smooth muscle cell motility. *Circ Res* **98**, 1381–1389.

Zhou H & Murthy KS (2003). Identification of the G protein-activating sequence of the single-transmembrane natriuretic peptide receptor C (NPR-C). *Am J Physiol Cell Physiol* **284**, C1255–C1261.

Zufall F, Ukhanov K, Lucas P & Leinders-Zufall T (2005). Neurobiology of TRPC2: from gene to behavior. *Pflugers Arch* **451**, 61–71.

Acknowledgements

This work was supported by operating grants from the Canadian Institutes of Health Research and the Heart and Stroke Foundation of Canada to W. R. Giles, and a Research Grant for Cardiovascular Diseases from the Japanese Ministry of Health and Welfare to Y. Imaizumi. R. A. Rose was supported by Doctoral Studentships from the Heart and Stroke Foundation of Canada and the Alberta Heritage Foundation for Medical Research. The authors thank Mr Lee Landeen for helpful discussions.